UNIVERSIDADE FEDERAL DO RIO GRANDE DO NORTE
PROGRAMA DE PÓS-GRADUAÇÃO EM NEUROCIÊNCIAS
INSTITUTO DO CÉREBRO
LABORATÓRIO DE NEURODINÂMICA

HERMANY MUNGUBA VIEIRA

INDICADORES DE CÁLCIO E DE VOLTAGEM CODIFICADOS GENETICAMENTE NA DETECÇÃO DE POTENCIAIS DE AÇÃO E INPUTS SINÁPTICOS EM CULTURA DE NEURÔNIOS HIPOCAMPAIS

Natal
2013

HERMANY MUNGUBA VIEIRA

INDICADORES DE CÁLCIO E DE VOLTAGEM CODIFICADOS GENETICAMENTE NA DETECÇÃO DE POTENCIAIS DE AÇÃO E *INPUTS* SINÁPTICOS EM CULTURA DE NEURÔNIOS HIPOCAMPAIS

Trabalho apresentado ao curso de Pós-Graduação em Neurociências da Universidade Federal do Rio Grande do Norte, como requisito parcial para a obtenção do Grau de Mestre.

Orientador: Prof. Dr. RICHARDSON NAVES LEÃO
Coorientador: Prof. Dr. MARCOS ROMUALDO COSTA
Neurobiologia Molecular e Celular

Natal
2013

HERMANY MUNGUBA VIEIRA

GENETICALLY ENCODED CALCIUM AND VOLTAGE INDICATORS IN THE DETECTION OF ACTION POTENTIALS AND SYNAPTIC INPUTS IN CULTURED HIPPOCAMPAL NEURONS

Dissertação apresentada ao curso de Pós-Graduação em Neurociências da Universidade Federal do Rio Grande do Norte, como requisito parcial para a obtenção do Grau de Mestre. Área de concentração: Neurobiologia Molecular e Celular

Apresentada em 04 de Março de 2013

BANCA EXAMINADORA

Prof. Dr. RICHARDSON NAVES LEÃO
UFRN

Prof[a]. Dr[a]. EMELIE KATARINA SVAHN LEÃO
UFRN

Prof. Dr. OLAVO BOHRER AMARAL
UFRJ

"The noblest pleasure is the joy of understanding."
Leonardo da Vinci

DEDICATION

To those on whose shoulders I can always cry, rejoice,
and climb to reach the highest. Mom and dad.

ACKNOWLEDGEMENTS

I am fully aware that all and any achievement I have conquered, or will, is grounded on the unconditional support I have been nurtured with for the past 25 years. Dad and mum, you have fostered my brain with music, laughs, and love, in a way that this is what comes out of me!

With all the differences, inside jokes and uncountable afternoons and nights playing Mario Kart, life in Natal would not have been half as fun without you Johnny and P'ana. Although our lives are taking divergent paths, I am sure it includes many mutual moments when we will share life – always with a laugh between photographs and memories.

Richie (Richardson Leão), with your intense and extravagant way of doing science, I must confess that I have learned what I didn't know existed. Brainstorm of new ideas, work done mingled with fun, and the love and enthusiasm that you exhale in the lab were some of the lessons. And they now reverberate in me and wherever else I will be being a scientist.

Marcos Costa, thank you for the final ideas on how to conclude my writings, figures; always with some time and a smile when I needed to ask you for something.

Kito (Markus Hilscher), sharing the rig room, our families and hometowns have been unexpected highlights of the last two years and it happened naturally, as our friendship effortlessly flourished and remains a "coisa linda".

Bru (Bruna Landeira) and Q (and Kelly Soares), without your friendship, guidance, our spontaneous hang-outs, deep conversations and exchange of so much advice, this journey would have had a flavor other than laughter, vows for our lives, and a type of affection I never expect to experience.

Carly Schott and Malte Kühnemund you were so far away, but still made yourselves the closest. And you directed my plans, making the big risks I had to take, worth it and safe. I moved to Sweden because I knew you would be there!

Daniel Zawadsky, you suddenly appeared standing in front of me, saying you would help me through the end of this long journey and you did it. Your company was essential.

To all the animals involved in this work, my respect and gratitude.

RESUMO

Neurônios se comunicam por meio de sinapses, trocando mensagens capazes de modificar o potencial de membrana de outros neurônios. Demonstrar o papel desses sinais e decodificar essa linguagem elétrica representa o grande objetivo da neurociência moderna. Atualmente, a eletrofisiologia é o ramo da neurociência capaz de investigar esses recursos elétricos de neurônios - que vão desde registros de condutância e comportamento cinético de canais iônicos individuais até a demonstração de neurônios individuais implicados em comportamentos complexos. Nesse sentido, diferentes estados cerebrais e comportamentos implicam o recrutamento de grandes conjuntos de neurônios se comunicando em um estado coerente, dinâmico. Além disso, essas grandes populações são formadas por diversos subtipos neuronais cuja análise requer ténicas que possibilitem uma resolução temporal e espacial de células individuais e, prefencialmente, de subtipos específicos. Apenas recentemente, indicadores ópticos geneticamente codificados surgiram como ferramentas não invasivas de alta resolução espacial e temporal utilizados para monitorar a atividade de neurônios individuais e populações neuronais específicas. O número crescente de novos indicadores optogenéticos, juntamente com a ausência de comparações em condições idênticas, gerou dificuldade em escolher a mais adequada das proteínas, dependendo do desenho experimental. Portanto, o objetivo deste estudo foi comparar três proteínas repórter recentemente desenvolvidas: os indicadores de cálcio GCaMP3 e R-GECO1, e o indicador de voltagem VSFP butterfly1.2. Foram expressos em neurônios do hipocampo em cultura, os quais foram submetidos a registros de patch-clamp e de imageamento óptico. Os três grupos (cada um expressando uma proteína) exibiram valores semelhantes de potencial de membrana (em mV, GCaMP3: -56 ± 8,0; R-GECO1: -57 ± 2,5; VSFP: -60 ± 3,9; p = 0,86), no entanto, o grupo de neurônios que expressam VSFP mostrou uma média mais baixa de resistência de entrada do que os outros grupos (em Mohms, GCaMP3: 161 ± 18,3; GECO1-R: 128 ± 15,3; VSFP: 94 ± 14,0; p = 0,02). Cada neurônio foi submetido a injeções de correntes com frequências diferentes (10 Hz, 5 Hz, 3 Hz, 1,5 Hz, e 0,7 Hz) e as suas respostas de fluorescência foram registradas. Em nosso estudo, apenas 26,7% (4/15) dos neurônios que expressam VSFP mostraram sinal de fluorescência detectável em resposta a potenciais de ação. O valor médio de sinal-para-ruído (SNR), obtido em resposta a cinco potenciais de ação (a 10 Hz) foi pequeno (1,3 ± 0,21), no entanto a cinética rápida do VSFP permite a discriminação de disparos, como picos individuais, com detecção de 53% dos APs evocados. Freqüências abaixo de 5 Hz, assim como variações no potencial de membrana subliminares, foram indetectáveis devido ao alto ruído do sinal de fluorescência. Por outro lado, os indicadores de cálcio mostraram maior alteração na fluorescência, seguindo o mesmo protocolo (cinco potenciais de ação a 10 Hz). Entre os neurônios expressando GCaMP3, 80% (8/10) exibiram sinal, com um valor médio de SNR de 21 ± 6,69 (soma), enquanto que para os neurônios expressando R-GECO1, 50% (2/4) dos neurônios demonstraram sinal com um valor médio SNR de 52 ± 19,7 (soma). Para protocolos de 10 Hz, 54% dos disparos foram detectados com evocado GCaMP3 e 85% com o R-GECO1. Disparos foram detectados em todas as frequências e os sinais de fluorescência foram também detectados a partir de despolarizações subliminares. Sendo GCaMP3 o indicador mais provável de produzir sinal de fluorescência e com alto SNR, alguns experimentos foram realizados somente com essa proteína. Observamos que GCaMP3 é eficaz na detecção de *inputs* sinápticas (envolvendo influxo de Ca^{2+}), com alta resolução espacial e temporal. Também foram observadas diferenças entre os valores de SNR resultantes dos disparos evocados, em comparação com os disparos espontâneos. Em registros de grupos de células, GCaMP3 mostrou clara discriminação entre células ativadas e silêncio, revelando-se como uma ferramenta potencial

em estudos de sincronização neuronal. Assim, nossos resultados sugerem que os indicadores de cálcio disponíveis atualmente permitem estudos detalhados sobre a comunicação neuronal, que vão desde dendritos individuais até a investigação de eventos de sincronia em redes neuronais geneticamente definidas. Em contraste, VSFPs representam uma tecnologia promissora para monitorar a atividade neural e, apesar de ainda requererem melhoramentos, podem se tornar mais apropriados do que os indicadores de cálcio, uma vez que os neurônios trabalham em uma escala de tempo mais rápida do que eventos de cálcio podem prever.

ABSTRACT

Recently, genetically encoded optical indicators have emerged as noninvasive tools of high spatial and temporal resolution utilized to monitor the activity of individual neurons and specific neuronal populations. The increasing number of new optogenetic indicators, together with the absence of comparisons under identical conditions, has generated difficulty in choosing the most appropriate protein, depending on the experimental design. Therefore, the purpose of our study was to compare three recently developed reporter proteins: the calcium indicators GCaMP3 and R-GECO1, and the voltage indicator VSFP butterfly1.2. These probes were expressed in hippocampal neurons in culture, which were subjected to patch-clamp recordings and optical imaging. The three groups (each one expressing a protein) exhibited similar values of membrane potential (in mV, GCaMP3: -56 ±8.0, R-GECO1: -57 ±2.5; VSFP: -60 ±3.9, p = 0.86); however, the group of neurons expressing VSFP showed a lower average of input resistance than the other groups (in Mohms, GCaMP3: 161 ±18.3; GECO1-R: 128 ±15.3; VSFP: 94 ±14.0, p = 0.02). Each neuron was submitted to current injections at different frequencies (10 Hz, 5 Hz, 3 Hz, 1.5 Hz, and 0.7 Hz) and their fluorescence responses were recorded in time. In our study, only 26.7% (4/15) of the neurons expressing VSFP showed detectable fluorescence signal in response to action potentials (APs). The average signal-to-noise ratio (SNR) obtained in response to five spikes (at 10 Hz) was small (1.3 ± 0.21), however the rapid kinetics of the VSFP allowed discrimination of APs as individual peaks, with detection of 53% of the evoked APs. Frequencies below 5 Hz and subthreshold signals were undetectable due to high noise. On the other hand, calcium indicators showed the greatest change in fluorescence following the same protocol (five APs at 10 Hz). Among the GCaMP3 expressing neurons, 80% (8/10) exhibited signal, with an average SNR value of 21 ±6.69 (soma), while for the R-GECO1 neurons, 50% (2/4) of the neurons had signal, with a mean SNR value of 52 ±19.7 (soma). For protocols at 10 Hz, 54% of the evoked APs were detected with GCaMP3 and 85% with R-GECO1. APs were detectable in all the analyzed frequencies and fluorescence signals were detected from subthreshold depolarizations as well. Because GCaMP3 is the most likely to yield fluorescence signal and with high SNR, some experiments were performed only with this probe. We demonstrate that GCaMP3 is effective in detecting synaptic inputs (involving Ca^{2+} influx), with high spatial and temporal resolution. Differences were also observed between the SNR values resulting from evoked APs, compared to spontaneous APs. In recordings of groups of cells, GCaMP3 showed clear discrimination between activated and silent cells, and reveals itself as a potential tool in studies of neuronal synchronization. Thus, our results indicate that the presently available calcium indicators allow detailed studies on neuronal communication, ranging from individual dendritic spines to the investigation of events of synchrony in neuronal networks genetically defined. In contrast, studies employing VSFPs represent a promising technology for monitoring neural activity and, although still to be improved, they may become more appropriate than calcium indicators, since neurons work on a time scale faster than events of calcium may foresee.

Key words: neuronal culture, patch-clamp, calcium imaging, voltage imaging

LIST OF FIGURES AND TABLES

ABBREVIATIONS

[Ca^{2+}]: calcium concentration

AP: action potential

Arch: Archaerhodopsin 3

ATP: adenosine triphophate

BSA: bovine serum albumin

CaM: calmodulin

CCD: charge-coupled device

CMV: cytomegalovirus

CNS: central nervous system

DAPI: 4' 6-diamidino-2-phenylindole

DIV: day *in vitro*

DMEM: Dulbecco's modified eagle medium

DNA: deoxyribonucleic acid

EGTA: ethylene glycol tetraacetic acid

ER: endoplasmic reticulum

EPSP: excitatory post-synaptic potential

FBS: fetal bovine serum

FP: fluorescent protein

FRET: fluorescent resonance energy transfer

GABA: gamma-aminobutyric acid

GAD: glutamic acid decarboxylase

GECI: genetically-encoded calcium indicator

GEVI: genetically-encoded voltage indicator

GFP: green fluorescent protein

GTP: guanosine triphosphate

HEK: human embryonic kidney

MAP-2: microtubule associated protein-2

NMDA: N-Methyl-D-aspartate

Osm: osmolars

P0: post-natal day 0

PCR: polymerase-chain reaction

PBS: phosphate buffer saline

PEST: penicillin streptomycin

ROI: region of interest

SD: standard deviation

SEM: standard error of the mean

SNR: signal-to-noise ratio

VSCC: voltage-sensitive calcium channels

VSD: voltage-sensitive dye

VSFP: voltage-sensitive fluorescent protein

YC: yellow cameleon

SUMMARY

"Scientists were skeptical about the usefulness of the microscopes. They would argue that everything one could see was just a matter of artifacts and a source of errors"
Santiago Ramón y Cajal. *Recuerdos de mi vida* (1917)

1 INTRODUCTION

Chapter I | When our minds started to mind

Curiosity has for thousands of years driven mankind to search for explanations on the uncountable questions encountered throughout ones' life. This mist of unknowns has allured men – desirous to unveil and perceive their own world. The surrounding immensity. The uncontrollable power of nature. The mysteries of our own body. In the course of time, men grew fascinated and determined to understand the fundaments of who we are. Explanations for dreams; origin of our emotions; the providing source for curiosity itself.

Although with divergent concepts emerging from time to time, the mentality that our brain constitutes the core of our intellect is not a recent belief. Back to Greece in the 4th century BC, Hippocrates came to a remarkable understanding on the human brain's role after his observations as a physician. He stated that:

> "Men ought to know that from nothing else but thence [from the brain] come joys, delights, laughter and sports, and sorrows, grieves, despondency, and lamentations." (Adams, F., 1886)

During the several following centuries, the restricted availability of techniques and tissue samples permitted advances mainly on anatomical descriptions of the central nervous system (CNS). Massive discoveries on the form and structure of the brain took place, also commonly fomenting rough suggestions for specific regions involved in certain functions or diseases. Thus far, however, nothing could be observed but what our eyes could see. And even supposing this overview to appear rather evident, this statement began to become obsolete with the advent of the first microscopes in the 17th century.

Cells were named and microorganisms could no longer live in secret. Combining techniques to develop better polished-lenses, together with the desire to contemplate the

minute parts of things, Robert Hooke and Anton van Leeuwenhoek were the first to explore the currently called microscopic world.

. . .

Not earlier than in 1836, Gabriel Valentin was the first to have a clear image showing a nerve cell (DeFelipe, 2010). At that time, microscope images could only be transposed from microscope lenses into the form of handmade drawings. Numerous optimized staining methods allowed a better visualization of neurons and their subparts, such as the nucleus and proximal projections. Microscope limitations and inadequate tissue preparations hampered the observation of the trajectory of dendrites and axons. It was not possible to be sure of how neurons were connected.

Among the several important names who developed new or improved old techniques, the Italian researcher Camillo Golgi was undoubtedly a remarkable one. In 1873, by the age of 30, Golgi published his silver nitrate method – which made full visualization of single neurons possible, in a way that detailed axons and dendrites could be viewed. For a reason still up to date unknown, his method only captures a random, small fraction of the neurons, which stand out in black from the majority of the unstained cells – as a yellow background. In Golgi's view, the brain comprised a continuous tissue sharing a single cytoplasm, as a network of anastomozed axons.

Years after the publication of the 'black reaction', as Golgi himself would call his staining, the Spanish histologist Santiago Ramón y Cajal came into contact with this innovative method, which redirected his interest to study the microscopic anatomy of the brain. In 1888, Cajal released his findings and drawings, from which he was confident to affirm that:

> "It could be said that each [nerve cell] is an absolutely autonomous physiological canton [unit]." (Ramón y Cajal, 1917)

According to Cajal's pioneering proposals, nowadays constituting the Neuronal Doctrine, the brain consists of complex, connected networks composed by separate, polarized cells whose communication has an established direction: the information flow goes from the dendrites of a neuron towards its soma and axon (for a review, Llinás, 2003). Beyond that,

Cajal also carefully examined the small protuberances running along neuronal dendrites (Figure 1). What at first sight he assumed to be technical artifacts, he at last named dendritic spines, foreseeing a physiological importance that the techniques at his disposal would not allow him to validate (García-Lopez, et al., 2007).

In a period when the curiosity about the brain's microarchitecture was confined to the investigation of unspecific, randomly stained, and lifeless neurons, the bedrock of cellular neuroscience emerged. And in parallel to the bright beginning of this neuroscience of single neurons, another revolution had already been launched: the electrical nature of the brain.

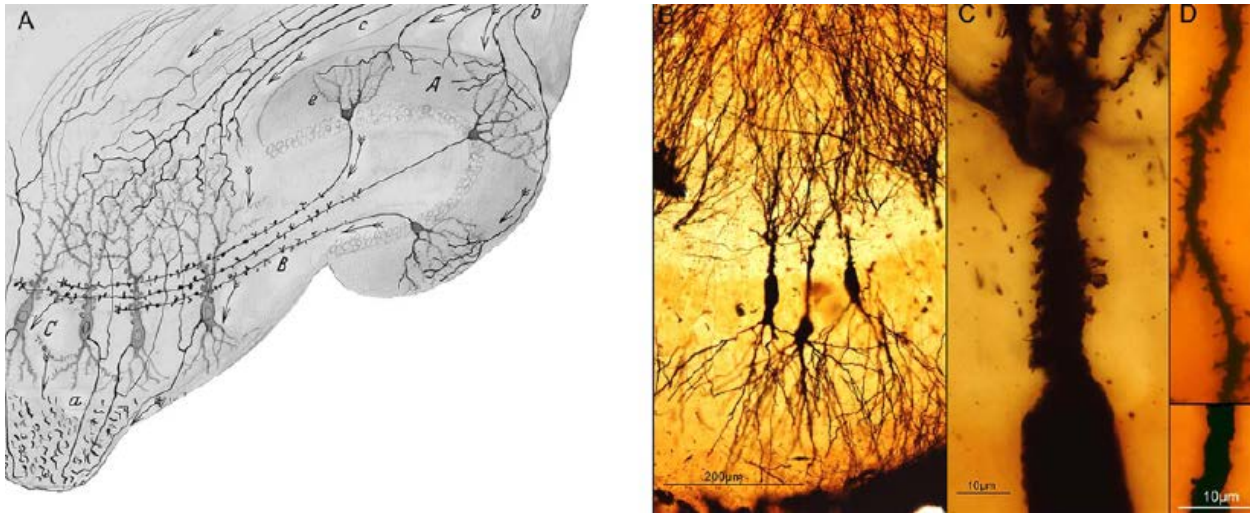

Figure 1 | Hippocampal dendritic spines: (A) Cajal's original drawing of hippocampal CA3 from a cat; Golgi stainings: (B) three hippocampal pyramidal cells; (C) apical process of a pyramidal cell; (D) a granule cell of cat hippocampus: upper segment with dendritic spines, while lower, without (from García-Lopez et al., 2007).

Chapter II | In charge of a lively neuroscience

In the very last years of the 18th century, a new era in the scientific scene sprouted. Luigi Galvani's work on frog muscles revealed that electricity belongs to the constitution of living beings. Already in the subsequent century, landmark discoveries occurred into the newborn field of electrophysiology. Electrical stimulation was used to determine functions of cortical areas; researchers executed the first recordings of electrical activity from the brain; the velocity of nerve impulse propagations were measured, and the first action potentials (APs) were registered from nerves (for a review, Verkhratsky, et al., 2006). However, the monitoring of the electrical properties of individual neurons demanded the development of sharper and smaller electrodes.

In the late 1930's, shortly after the discovery of cells' bilayer lipid membrane, Alan Lloyd Hodgkin and Andrew Huxley were the first to successfully record electrical activity from the membrane of single neurons (Hodgkin and Huxley, 1939). Using the recently developed voltage-clamp technique, they were able to reveal the biophysical mechanisms of APs (Hodgkin and Huxley, 1952a, b, c). Ongoing improvements rapidly allowed researchers to perform single channel and intracellular recordings, although up to this time, muscle fibers and giant axons were the only sufficiently large cells, suitable for electrophysiological experiments.

In 1976, Erwin Neher and Bert Sakmann succeeded in electrically isolating a patch of muscle fiber membrane and recognized the extremely low noise originated by this small membrane portion. It not only made possible the measurement of currents at the scale of picoamperes, but also the functional characterization of single ion channels (Neher & Sakmann, 1976). Their work marked the establishment of the patch-clamp technique and the redirection of electrophysiologists' interest towards the small, now approachable, mammalian neurons.

The patch-clamp technique

Neurons communicate trading messages. Intercellular messages which modify the membrane potential of other neurons. Demonstrating the role of these signals to thus decode this electrical language embodies the utmost goal of modern neuroscience. At the present time, electrophysiology represents the branch of neuroscience able to explore these electrical

features of living neurons – ranging from recordings to investigate the conductance and kinetic behavior of single ionic channels (Banks and Pearce, 2000) to the demonstration of individual neurons implicated in complex animal behaviors (Lapray et al., 2012).

Exploiting the possibility to control either the membrane potential or the currents passing through neuronal membranes, the development of the patch-clamp techniques generated unprecedented new approaches to study the CNS. Over the past 30 years, improvements covered all steps of a patch-clamp experiment: fire-polished glass pipettes with custom low resistances, low-noise amplifiers, ideal electrolyte solutions, higher seal resistances (allowing a better electrical isolation of the membrane patch), in addition to maximized signal-to-noise ratio (SNR) from the electrical recordings (Hamill et al., 1981).

In general lines, two categories comprise the main conditions for patch-clamp experiments. In the voltage-clamp condition, the membrane potential of the neuron is held constant and thereby it is possible to measure small currents generated by ions moving across the neuron's membrane. For example, it is possible to spot the ion channels expressed in a certain cell, to study responses to specific pharmacological agents, as well as the monitoring of currents from excitatory post-synaptic potentials (EPSPs). The second patch-clamp mode is the current-clamp, in which the membrane voltage can freely vary, in such a way that it allows the measuring of APs and subthreshold depolarizations with very high spatial-temporal resolution and sensitivity. With its diverse possible configurations, patch-clamp methods offer the possibility to probe different facets of neuronal function. Neurons from potentially any region of the brain, of various species, and in different stages of development can be carefully studied with these techniques.

A widely explored patch-clamp preparation consists of dissociated neuronal cultures, which provide high-quality visualization and access to individual cells (Rouach et al., 2003; Kuczewski et al., 2008, Mah et al., 2011), yielding powerful insights on the structural and electrophysiological profile of specific types of neurons *in vitro*. Brain slices, on the other hand, represent an improved alternative to gain knowledge about connectivity of neurons in their reasonably preserved anatomical constitution (Leão et al., 2012). Additionally, patch-clamp recordings can now be obtained from several different neurons simultaneously (Perin et al, 2011) and from different compartments of the same cell, such as soma, axon, and dendrites (Kole, 2011). Moreover, it is possible to record from both pre- and postsynaptic neurons from cultures or brain slices and thereby investigate the role of individual cells in a

neuronal network (Leão et al., 2012). Moreover, by modifying the composition of the bathing solutions by changing ion concentrations or adding specific pharmacological agents, researchers have the ability to controllably manipulate and dissect neuronal physiology – one of the greatest advantages of *in vitro* experiments.

Nowadays, patched cells can also be recorded from *in vivo* preparations. Not just from anesthetized animals (Portez & Larkum, 2008); recently, specialized laboratories have developed the challenging expertise of recording from freely moving, drug-free rodents (Lee, et al., 2006; Lapray et al., 2012), with which a great deal of knowledge has been and will be obtained in respect to individual neurons pacing complex, intricate behaviors.

Optical monitoring of neurons

Brain states and behaviors involve the recruitment of not only different, but also large neuronal ensembles communicating in a dynamic, coherent state. For decades, neuronal populations have been investigated with a variety of traditional methods, such as electroencephalography and local field potentials (Buzsáki et al., 2012), where such classical electrophysiological strategies of large-scale recordings have generated important links between neuronal assemblies and specific behaviors (Buzsáki 2004). And although large populations can be analyzed with such techniques [e.g. multi-electrode arrays (Einevoll et al., 2012)], there is barely no spatial resolution regarding the individual cells registered, leaving imprecise the role played by single neurons among the large populations assessed.

To investigate neuronal functions at a circuit level, optical imaging allowed not only the monitoring of large neuronal populations in high single-cell resolution, but also the study of biophysical events occurring at neuronal structures unreachable with traditional electrophysiological approaches, such as recordings from dendritic spines (Nimchinsky et al., 2002). In other words, the use of fluorescence methods enabled neuroscientists to study the activity of both single or multiple neurons with outstanding temporal and spatial resolution (Grinvald & Hildescheim, 2004), capable of resolving even small segments of neurons (Ji et al., 2008).

Decades have passed since the earliest organic fluorescent dyes started to be used to enlighten the mysteries of neural networks (Tasaki et al., 1968; Salzberg et al., 1983). Because of their vast flexibility, imaging methods can faithfully report diverse physiological

events, such as pH variations, as well as changes in ion concentrations and in membrane potential. Combined with new technologies in microscopy, these optical reporters have been applied in a wide spectrum of studies on neuronal dynamics: plasticity at the level of dendrites (Nimchinsky et al., 2002), neuronal assemblies of ongoing cortical activity (Arieli et al., 1995), and insights on the development of the neocortex (Polley et al., 2004).

The most widely employed strategies consist of using voltage sensitive dyes (VSDs) and calcium-sensitive dyes, compounds sensitive to changes in membrane potential and intracellular calcium concentration ($[Ca^{2+}]$) respectively. VSDs consist of lipophilic substances that bind to cellular membranes and, in response to voltage changes, produce voltage-dependent fluorescent signals (Grinvald & Hildesheim, 2004). The gold standard of VSD provides signals as fast as the membrane potential time scale, fluorescence changes linearly correlated to membrane potential, and reliable optical detection without the need of averaging (Bradley et al., 2009). Among the several significant findings achieved with the use of VSDs (for a review, Grinvald & Hildesheim, 2004), some highlights are: optical recordings of cortical representations of whisker touch in freely moving mice (Ferezou et al., 2006), studies on input integration in the sensorimotor cortices (Ferezou et al., 2007), and long-term studies of cortical dynamics in non-human primates (Slovin et al., 2002).

Changes in $[Ca^{2+}]$ own a central role in intracellular cascades activated during neuronal activity. Fluorescent molecules responsive to Ca^{2+}, known as calcium-sensitive dyes, constitute the second major class of organic dyes and have been useful tools to detect both supra- and subthreshold events (Svoboda et al., 1997; Fetcho et al., 1998), such as synaptic inputs arriving in individual dendritic spines (Sabatini & Svoboda, 2000) exemplifying their powerful applicability to study synaptic activity and neuronal plasticity. Despite their great success and wide usage, this group of dyes provides a time scale that is too slow for consistent detections of AP trains at higher frequencies (Dombeck et al., 2007), mostly because it relies on the slow time course of neuronal Ca^{2+} dynamics itself. A complementary alternative is to combine voltage and Ca^{2+} dyes covering non-overlapping fluorescence spectra, consisting of a powerful strategy to concomitantly investigate APs with excitatory synaptic inputs at high rates (Berger et al., 2007).

Despite the immeasurable contributions achieved with the use of the numerous available dyes, a range of experimental conditions and questions remain impossible to be addressed with fluorescent dyes. The most limiting drawback consists of the lack of neuronal

population selectivity. When seeking to investigate the role of specific subpopulations of detailed circuits, the use of organic dyes becomes unsuitable due to its ubiquitous staining of unidentified cells. On top of that, when labeling all the cells in a tissue, the background fluorescence increases, which therefore lowers SNR values. Still in that regard, organic dyes are also not specific to the plasmic membrane and can aggregate to internal membranes, such as the endoplasmic reticulum (ER), also increasing background noise (Scanziani & Häusser, 2009). Furthermore, because of their commonly high toxicity and photobleaching, experiments can hardly last for periods longer than hours, hampering chronic experiments to be performed (for an important exception, Slovin et al., 2002).

Instead of having large, unspecific groups of neurons imaged, another possibility is to optically record single neurons. By patching individual cells with a pipette filled with a fluorescence dye, one can perform simultaneous multisite optical monitoring of different segments of the same cell (Bradley et al., 2009). Furthermore, by loading not one, but a few neurons that occupy the same layer/subregion of a brain slice, one can look into the concomitant activity of small subsets of related cells and associate electrophysiological attributes to a reasonably defined neuronal population. Nevertheless, this consists of an exceptionally laborious technique where in many cases dye loading takes from 30 min to 1 hour; in addition, as the experimenter waits for the dye to load, the patch-pipette has to be removed from the neuron, as the dye and the cytoplasm of the cell would diffuse back to the pipette. This procedure is highly harmful and often leads to neuronal death.

At this moment, however, a resulting question remains to be answered: who are these neurons? In order to identify or to confirm the subtype of neurons optically recorded, a toolbox for post-hoc labeling techniques is available and is briefly discussed below.

A molecular tag

A high-quality view of individual neurons became possible with the advent of neuronal cultures; the study of subregions of the CNS is achievable by probing brain slices; and more recently *in vivo* experiments enabled the investigation of individual neurons' activity in their intact morphology, connectivity, and constitution. However, neuronal circuits are composed by a variety of tangled types of neurons, in a way that when studying brain networks it is indispensable to exploit methods through which specific groups of cells can be distinguished and defined. Surprisingly, sorting neurons in well-defined categories is still up to date a matter of debate and/or personal preference. There are classifications dividing

neurons by their embryonic origin, adult morphology, neurotransmitters released, projecting processes, electrophysiological properties, etc. Among the many parameters previously and currently utilized, one of the most powerful is the molecular profiling of neurons, founded on the unique expression of their genes and proteins.

The use of molecular markers has at least two main applications in the study of neuronal subtypes. The first considers the expression of constitutively expressed genes, i.e., genes continually transcribed. Such 'static markers' can be sought in order to determine subclasses of cells, which will be defined by the presence or lack of the specific elements investigated. As an example, the expression of the enzyme glutamatic acid decarboxylase (GAD), which synthesizes the neurotransmitter gamma-aminobutyric acid (GABA), assigns every GAD-expressing neuron as GABAergic. Although apparently simplistic, such general classifications allowed initial delimitations of neuronal populations. Within the GABAergic class of neurons, for example, even if considering only other molecular markers (and neglecting electrophysiological/morphological features), dozens of other subclasses can be classified by their differential expression of other proteins, such as parvalbumin-, somatostatin-, calbindin-positive GABAergic neurons.

A second application for molecular markers focuses on the expression of facultative genes, i.e. genes only transcribed at defined episodes or as a result of specific cellular activities. Therefore, the expression of such molecules can be used as a byproduct of certain cellular functions and be assumed as an indirect indicative of the occurrence of defined cellular events in a determined time interval, such as in studies searching for immediate early genes (e.g. c-Fos, c-myc, Arc), as one example.

The combination of patch-clamp methods with subsequent labeling of the cells enables experimenters to classify subtypes of neurons with common parameters at the molecular, morphological and electrophysiological levels (Ryge, et al., 2008). For monitoring both temporary and continued expression of genes, a variety of techniques are available, such as immunohistochemistry, *in situ* hybridization, reverse-transcriptase PCR, avidin-biotin complex, etc; each carrying particularities that will make them best suitable for different questions.

Chapter III | Reporting activity with genetic codes

The era when circuit-centered quests can be addressed in living neurons began in the early 1960's when Osamu Shimomura started searching the source for the glow of the jellyfish *Aequorea victoria*. The discovery, purification (Shimomura et al., 1962; Morise et al., 1974), and future cloning (Prasher et al., 1992) of the bioluminescent protein, hereafter named green fluorescent protein (GFP), provided the revolutionary opportunity to genetically label different cell subtypes without the need for fixation and exogenous, labeling agents.

Studies on the biochemical properties of the GFP demonstrated that the structure of its chromophore (portion of a molecule responsible for its color) does not require cofactors or external enzymes (for a themed review see, Tsien, 1988). This characteristic of spontaneous protein folding allowed the introduction of GFP within a wide range of different species. In further studies for optimizing its biosynthesis within mammalian cells, a range of directed single amino acid mutations were implemented and yielded increased folding rate, optimized maturation at 37°C, higher protein stability, resistance to pH variations, and prevention of oligomerization (for a review, Kremers et al., 2011). Several key mutations were also widely exploited for the development of new fluorescent proteins (FPs) covering different light spectra (for a review, Daya and Davidson, 2009), expanding to colors reaching up to the orange, red and far-red spectral zones (Shaner et al., 2008; Shcherbo et al., 2009).

With specific promoters, FP expression can be directed, temporally determined, and boosted in defined cell populations, as well as used to quantify other proteins (1:1 ratio) when its expression is made dependent on the synthesis of other proteins. Plenty of other modern alternatives allow scientists to express a fluorescent reporter under the control of a known promoter, by using viral vectors, electroporation techniques, and transgenic lines, such as a mouse line for glutamatergic neurons (Borgius et al., 2010).

The fluorescence properties of the FPs are highly dependent on the surrounding physicochemical environment within a cell, so that disturbances in the cellular milieu can produce conformational changes with variations in brightness, photostability, and even spectral shifts (Kremers et al., 2011). Over the last 15 years, protein engineering enabled the fusion of FPs with proteins known to respond to specific physiological variations guiding the generation of the state-of-the-art approaches in optical imaging: optogenetic indicators that enable queries for activity changes at subcellular compartments in large populations of genetically identified cells (Mutoh & Knöpfel, 2013).

This class of pioneering molecules is basically composed of two fused proteins. The first acts as a biosensor that detects variations related to a specific physiological event (for example [Ca^{2+}], pH, and voltage changes), determining the sensitivity of the reporter. Changes in the physiological parameter will cause a conformational change in the sensor domain and will cause the second protein, which is fluorescent, to convert the detected physiological signals in variations of fluorescence emission (Knöpfel, 2012). For example, the GCaMP3 (one of the calcium-indicator used in this study) consists of a calmodulin (CaM) domain – an endogenous calcium-sensitive protein – fused to GFP, as the fluorescent reporter (Tian et al., 2009). The M13 peptide (derived from skeletal muscle myosin light chain kinase) is included to enhance conformational changes and increase fluorescence readouts.

Trends in neuroscience

Neuronal signals occur within the timescale of milliseconds, which makes the recording of neuronal activity, with effective space and time precision, a major goal and priority in neuroscience. In that regard, genetically encoded, optical reporters have recently emerged as high spatial and temporal resolution tools for monitoring the activity of neurons. Compared to fluorescent dyes, optogenetic tools induce much lower or no toxicity; allow a stable, long-term expression of the reporters in potentially any aimed, large-scale neuronal population possible to be fully recorded at once. Targeting those indicators to defined neural populations allows the study of large numbers of cells of one type, with ongoing improvements seeking for the potential independence on electrode-based recordings.

Genetically-encoded indicators are commonly composed of two fused proteins, whose designs are based on two main configurations: I) a single FP fused to a sensor protein by a short spacer; or II) two different FPs having their fluorescence emission based on fluorescent resonance energy transfer (FRET) – which consists of a physical process of energy transfer from a donor chromophore (at its excited state) to an acceptor chromophore; a phenomenon strongly dependent on the orientation and distance between the two fluorescent molecules. Conformational changes in the sensor-protein of such indicators will modify the distance between the two FPs and, in consequence, evoke variations on the FRET readout.

Genetically-encoded voltage indicators (GEVI) and genetically-encoded calcium indicators (GECI) are the most widely used probes in modern neuroscience (Scanziani & Häusser, 2009; Knöpfel, 2012) and will be further addressed in this study.

VOLTAGE INDICATORS

Neuronal membrane potential provides information about synaptic inputs, APs, and cellular communication. Monitoring voltage fluctuations in neurons can be achieved using GEVIs, which detect variations in membrane potential and convert them into fluorescent signals. The design of first GEVI consisted of a modified green fluorescent protein (GFP) fused to a voltage-sensitive K^+ channel (Siegel & Isacoff, 1997), expressed and exploited in oocytes. However it was only after 10 years that an efficiently optimized probe was released (Dimitrov, et al., 2007) and currently composes one of the best up-to-date classes of GEVIs, known as voltage-sensitive fluorescent proteins (VSFPs) (Sakai, et al, 2001; Dimitrov, et al. 2007, Mutoh, et al. 2009, Akemann, et al. 2012, Perron, et al. 2009).

VSFPs are engineered proteins that reside in the membranes of neurons and provide the link between fluorescent and activity reporters. They are based in the concept of structural rearrangements of voltage-gated ion channels or isolated voltage-responsive domains, coupled to a pair of fluorescent proteins; whenever a neuron receives a signal, the resulting variation in voltage potential in the cell membrane leads the VSFPs to rearrange into a configuration that causes a readily detectable change in the optical signal generated by the FRET (Akemann et al., 2010).

The first prototype of VSFP was based on a voltage dependent K^+ channel subunit, fused to a pair of cyan and yellow fluorescent proteins (Sakai et al., 2001). This probe successfully reported changes in membrane potential, but showed poor targeting to the plasma membrane of mammalian cells. Several VSFPs have been developed with promising variants based in a voltage-sensor phosphatase derived from the sea squirt *Ciona intestinalis*. This new class was named VSFP2 and includes constructs composed of a four-transmembrane voltage domain (S1-S4), coupled to a pair of fluorescent proteins, exhibiting improved targeting to the plasma membrane (Akemann, et al., 2010; Knöpfel, et al., 2010). Another configuration was called VSFP3 and makes use of a single FP instead of a pair of FRET-based FPs (Perron et al., 2009). The advances of using a single FP concern a faster

kinetics and availability to use a broader color spectrum. Despite these promising advantages of VSFP3s, it displayed smaller signal amplitudes compared to VSFP2 (Perron, et al., 2009).

The variant VSFP2.3 was the first extensively applied GEVI which allowed the optical imaging of APs in brain slices and *in vivo*; more importantly, it enabled imaging of APs without averaging multiple trials (Akemann et al., 2010), although only in brain slices. Nevertheless, the authors have also shown macroscopic representations of layer 2/3 pyramidal cells expressing VSFP2.3 responding to whisker deflection.

In 2012, two new GEVIs were published. The first probe of a new class of voltage indicators was named Archaerhodopsin 3 (Arch), consisting of a microbial opsin–based voltage sensor, from *Halorubrum sodomense*, whose fluorescence is associated to protonation of a rhodopsin (Kralj et al., 2012). Although dimmer than VSFPs, Arch resolved individual spikes and demonstrated fast speed and high SNR when expressed in cultures of hippocampal neurons. The second recently released reporter, alternatively, is the most recent member of the vast class of VSFPS. On its novel design, they are called VSFP-butterfly and combine the properties of larger dynamic ranges of VSFP2s with fast kinetics of VSFP3s (Perron et al., 2012). In this configuration, the voltage sensor domain is sandwiched between two fluorescent proteins that undergo FRET upon activation. Two types of VFSP-butterflies were developed; one composed by mCerulean and mCitrine (VFSP-butterfly1.0) and the second by mCitrine and mKate2 (VFSP-butterfly1.2). They are currently the best performing VSFPs and have been used to report in good temporal precision the spread of subthreshold oscillations *in vivo*, with good precision and with high membrane targeting (Akemann et al. 2012).

CALCIUM INDICATORS

The toolbox of GECIs is composed of engineered fluorescent proteins that can be targeted to specific cell populations in order to monitor changes in $[Ca^{2+}]$. The pioneer of this family was published in 1997 (Romoser et al., 1997), nowadays symbolizing a premature version of the latest, highly superior new versions of GECIs. Many of the state-of-the-art current probes, such as GCaMP3 and GCaMP5 (see below), still possess the original, but refined framework of the first prototype: GFP fused with a calcium-binding domain of the protein CaM.

The most recently developed GECIs have undergone several improvements and nowadays exhibit powerful features that make them potent strategies for studies in the mammalian brain. Currently, there are two main classes of GECIs (for a review Mank & Griesbeck, 2008). All the proteins encompassing the first group contain a Ca^{2+}–sensitive CaM domain linked to two different possible fluorescent configurations: either a single circularly permutated fluorescent protein [such as GCaMPs (Tian et al., 2009; Akerboom et al., 2012) and GECOs (Zhao et al., 2011)] or a FRET-based pair of FPs, composing the family of 'yellow cameleons' (YC) (Horikawa et al., 2010). Alternatively, the second class of GECIs relies on a different calcium molecule, troponinC, a protein not endogenously expressed in neurons (only in muscle cells) and, therefore, believed to reduce possible interactions with Ca^{2+}-sensing cellular targets when compared to CaM, which is expressed in neurons.

Massive improvements during the past decade enabled the use of GECIs in a wide range of experimental approaches (for a review, Tian et al., 2012). Remarkably, variants of all classes have been shown to be functional *in vivo*: the troponinC-containing protein TN-XXL (Mank et al., 2008), as well as YC3.6 (Lütcke et al., 2010), the high Ca^{2+}-affinity YC-Nano15 (Horikawa et al., 2010), and GCaMP3 (Tian et al., 2009).

The most widely used subclass of GECIs, however, has been the family of the GCaMPs. Through sequential cycles of optimization, directed by the known structure of the subtype GCaMP2, researchers were able to increase protein stability, baseline brightness, and dynamic range (Tian et al., 2009). The resultant new construct, GCaMP3, allows the detection of APs by line-scanning pyramidal cell dendrites (in terms of detectable signal, not individual spikes); furthermore, it has been possible to detect from 3 to 10 APs of cortical neurons in behaving mice, although always evoked at high frequency trains (~80 Hz), without discrimination of individual spikes (just SNR amplitude). Thus, GCaMP3 clearly exhibits improved properties for detection of large numbers of APs, because of its high dynamic range and high fluorescence signals; however, the kinetics of GCaMP3 is still relatively slow and was not proven suitable for detection of single APs.

Not until recently, all single FP-based calcium indicators were based on green variants of GFP. By using mutagenesis and genetic screening of bacteria colonies on the GCaMP3 construct, new variants were developed and now compose an expanded palette of colorful calcium-indicators (Zhao et al. 2011). The new engineered probes include FPs

covering the spectrum of blue, an improved green version, and, most importantly, the first red-shifted GECI, based on the substitution of the GFP by the far-red shifted protein, mApple. Named R-GECO1, this red calcium-indicator maintained similar kinetics properties of the GCaMP3, but with improved signal amplitudes in terms of response to Ca^{2+} changes (Zhao et al. 2011). The use of longer wavelength light excitation (red spectrum) instead of the blue-shifted spectrum represents a preferable choice, for its significantly lower phototoxicity and deeper tissue penetration when performing calcium imaging *in vivo*.

Fluorescence responses to [Ca^{2+}] changes are critically dependent on the affinity, kinetics, and dynamic range of the selected probe. Depending on the application of GECIs, researchers can focus their question on either detecting sparse APs, dynamic range (amplitude) after spike bursting, or temporal discrimination of individual APs (Tian et al., 2012). Very recently, a family of new GCaMP variants was published with the aim of making available multiple versions with specific improved performances, named the GCaMP5s (Akerboom et al., 2012). Compared to GCaMP3, their main achievements are related to increase in fluorescence baseline and range, as well as the fact thatone of the probes (GCaMP5K) enables the detection of single spikes (*in vitro*).

One of the main advantages of using genetically-encoded indicators of neuronal activity is the possibility of long-term expression for performance of chronic experiments. When GCaMP3 was chronically expressed (months) in chemosensory neurons in *Caenorhabditi. elegans*, no detected cytotoxicity or behavioral changes were observed, with maintained high expression of the probe (Tian et al., 2009). Conversely, behavioral impairments have been seen with the expression of other GECIs (Tian et al., 2009; Tian et al., 2012), proving the importance of the development of nonfunctional indicators under reliable evaluations. In that regard, helpful mouse lines have recently become available, allowing stable, long-term expression of GCaMPs, driven by different genetic strategies (e.g., Cre lines) in promoter-specified neuronal populations (Chen et al., 2012; Akerboom et al., 2012; Zariwala et al., 2012).

2 RATIONALE

Understanding neuronal networks will require the ability to monitor APs and synaptic activity in identified neuronal populations. However, the increasing number of optogenetic reporters, combined with the lack of comparisons under identical conditions, has generated the difficulty of choosing the most appropriate probe for assessing activity of individual neurons or networks.

While GEVIs provide faster kinetics and are able to detect single APs at higher frequencies (although with significant lower signals), GECIs provide larger dynamic ranges and, hence, higher SNR compared to the voltage-reporters; their properties also enable the monitoring of subthreshold activities associated to synaptic inputs, although no studies have investigated spontaneous *versus* evoked APs. Therefore, both classes of genetically-encoded indicators endow different advantages/disadvantages and, up to date, no study has compared these two major classes of neuronal activity reporters.

Here, we chose to compare GCaMP3 (as the most widely established and employed GECI), R-GECO1 (for its far-red shifted fluorescence), and the voltage-indicator VSFP Butterfly 1.2 (for its fast kinetics and also red-shifted fluorescence) under similar experimental conditions. These constructs were expressed in cultured hippocampal neurons in order to assess their fluorescence emission readouts in response to membrane potential variations resulting from synaptic inputs and APs at different frequencies.

3 OBJECTIVES

3.1 General

To compare three genetically-encoded activity indicators on the detection of neuronal activity in cultured hippocampal neurons.

3.2 Specific

- To implement the technique for neuronal cultures expressing the genetically-encoded indicators studied;
- To investigate if the expression of the probes determine changes in fundamental electrophysiological properties of the neurons in culture;
- To compare fluorescence readouts in response to evoked APs;
- To monitor and evaluate the fluorescence signal of probe-expressing neurons in different frequencies for spike detection;
- To compare fluorescence signals from evoked and spontaneous APs;

"It's no longer enough for a man to say that something is so
or how it is so – everything now has to be proven besides, preferably
with witnesses and numbers and one or another of these […]
experiments."
Patrick Süskind. ***Perfume, the story of a murderer***

4 METHODS

4.1 Mouse Breeding

Mice were raised under standard animal housing conditions in a 12h light/dark cycle with food and water available *ad libitum*. All experiments were performed in accordance with the European Communities Council Directive (86/609/EEC) and were approved by the appropriate Swedish Ethical Committee (Uppsala Animal Ethics Committee, Jordbruksverket) and the Comitê de Ética no Uso de Animais da UFRN (CEUA 013/2012) .

4.2 DNA Purification

We used plasmids containing cDNA for VSFP Butterfly 1.2 (VSFP1.2) (gift from Thomas Knöpfel's laboratory), R-GECO1 (Addgene plasmid #32444) and GCaMP3 (Addgene plasmid #22692), under the control of a CMV-promoter, which allows expression in all mammalian cell types.

Chemically competent bacteria (DH5α) were transformed with each of the vectors by heat shock and grown overnight at 37°C on agar plates with 10 ug/ml ampicillin for VSFP1.2 and R-GECO1, and 50 ug/ml kanamicin for GCaMP3. Single colonies were picked and amplified in 250 ml of standard LB medium with 1% ampicillin or kanamycin with overnight shaking at 32°C.

DNA was purified using HiPure Plasmid Purification Systems (Invitrogen #K2100-07) using optimized instructions from manufacture. The concentration and the purity of the amplified vectors were measured by a NanoDrop Spectrophotometer (NanoDrop Technologies). DNA purity reached values higher than 95% with DNA concentrations of >1ug/ul.

4.3 Cell Culture

4.3.1 HEK cells

HEK293 cells were grown in complete DMEM, composed of high glucose DMEM (Invitrogen #11965-092) with 10% Fetal Bovine Serum (FBS; Invitrogen #16000-044) and 1% PEST (100 U/ml Penicillin + 100 mg/ml Streptomycin; Invitrogen #15140-148) at 37 °C, 5% CO_2. Cells were passed two days pre-transfection and grown until the confluence reached 90%. A few hours pre-transfection, growth medium were changed to RPMI-1640 serum free medium (Invitrogen #22400-105).

We transfected HEK cells only with the VSFP1.2 plasmid using the TrueFect-Lipo kit (United BioSystems #TF1101-1), following instructions from manufacture. Transfected cells were plated on cover slips coated with poly-L-lysine (Sigma #P2636) and analysis of expression was performed 48 hours post-transfection. Current-clamp recordings were performed in order to determine an optimized set of excitation/emission filters, as well as the best configuration for data acquisition. Among eight cells, one evoked fluorescence signal in response to changes in membrane potential, indicating that the configuration was sufficient for data collection in neurons (Fig. 2).

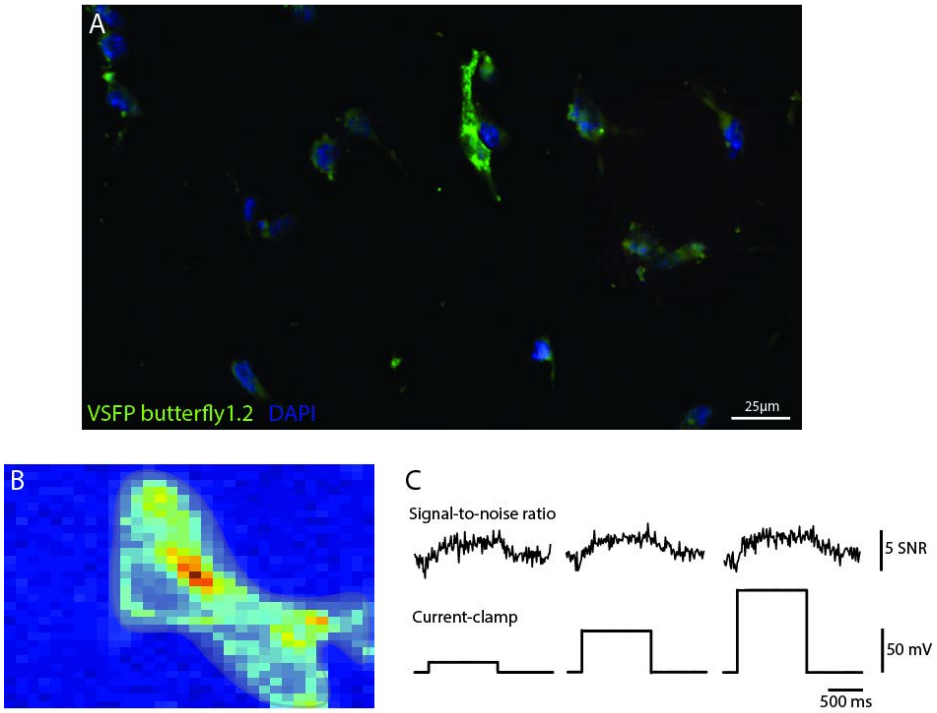

Figure 2 | Current-clamp and voltage imaging of HEK cell expressing VSFP butterfly1.2. (A) Fluorescent image (only for the fluorescent protein Citrine) of HEK cells expressing VSFP1.2 with nuclei labeled in blue with DAPI; (B) Fluorescence representation patched HEK cell and selected ROI. (C) Signal-to-noise ratio values correspond to the evoked membrane depolarizations showing no ratiometric variations corresponding to the membrane potential changes. ROI: region of interest.

4.3.2 Primary Hippocampal Cultures

Primary cultures of hippocampal neurons were prepared from P0-P2 mouse pups. Hippocampi were dissected in sterile, ice-cold phosphate buffer saline (PBS) 10mM glucose. After that, isolated hippocampi were transferred to a digestion solution of 0.125% trypsin (Invitrogen #25300-054) for 30 min at 37°C. In order to stop the action of the trypsin over the hippocampi, the digestion solution was aspirated and we added medium containing FBS (same content of HEK cells medium), once its protein content is believed to stop the activity of the enzyme over the hippocampi by competition. With glass pipettes of different apertures, the still intact hippocampi were mechanically triturated until the solution was homogeneous.

Subsequently, cells were counted with Trypan Blue (Invitrogen #15250-061) in a Neubauer chamber (1:1) to count and check the ratio of healthy *versus* dead cells. Neurons were centrifuged (5 min at 300 rpm); resuspended with 100 ul of the Mouse Neuron Nucleofector Solution (Lonza #VPG-1001); mixed with 2-3 ug of DNA (VSFP1.2, R-GECO1 or GCaMP3); and then transfected using the Nucleofector (Amaxa™ Nucleofector™ Technology). The resulting cell suspension was diluted (~10^5 cells/ml) with complete high glucose DMEM and seeded in 24-well cell culture plates (1 ml/well) with cover slips pre-coated with both poly-L-lysine and laminin (Sigma #L2020). After 4h at 37°C in a humidified incubator maintained with 5% CO_2, the plating medium was substituted by Neurobasal medium (Invitrogen #21103-049), supplemented with 2% B27 (Invitrogen #17504-044), 2 mM GlutaMAX (Invitrogen #35050-061), and 1x PEST.

In parallel, some cells did not undergo transfection and were simply plated in complete DMEM, afterward replaced by supplemented Neurobasal. With 2-3 days *in vitro* (DIV), non-transfected cultures received 1 ul of AAV2/9.hSynap.GCaMP3.WPRE.SV40 (PennVector #AV-9-PV1627) in order to ensure extremely high percentage of transduced neurons (~100%) for experiments of groups of cells (see Section 5.4.3). Cultures were kept at 37°C in 5% CO_2 (7-28 DIV), when patch-clamp and imaging recordings were executed.

4.4 Immunocytochemistry and expression analysis

After experiments, some neuronal cultures were fixed with paraformaldehyde (4%) for 5 min at room temperature. After three times rinsed with PBS, 0.1% Triton-X in PBS was added for 15 min and then washed with PBS. To block nonspecific binding sites, cover slips

were incubated for 2h with blocking solution composed of 5% NGS (Normal Goat Serum; Invitrogen #PCN5000) and 0.1% Triton-X in PBS.

Cultures received the primary antibody solution (1:500 – diluted in blocking solution), followed by overnight incubation in a humid chamber at 4°C. After three washes (10 min PBS), cells received the secondary antibodies (1:1000) and were incubated in a humid chamber in the dark at room temperature.

Two primary antibodies were used as markers for neuronal maturation: mouse monoclonal anti-MAP-2 (microtubule-associated protein 2) (Sigma #M1406), selective to the neuronal soma and dendrites; and mouse monoclonal antibody anti-synapsin-1 (SySy #106-001), a pre-synaptic marker for synapses. Secondary antibodies used were Alexa Fluor® 546 Goat Anti-Mouse IgG1 (Invitrogen #A-21123) and Alexa Fluor® 488 Goat Anti-Mouse IgG (Invitrogen #A-11001). Following the secondary antibody staining, cover slips were again washed three times with PBS, followed by administration of DAPI (1:1000) in PBS for 5 min, in order to stain the nuclei of the cells. After a final step of two more washes with PBS, the cover slips were mounted with Mowiol 4-88 (Sigma #81381).

Confocal microscopy was done using the Zeiss LSM 510/Laser Module, equipped with x10, x20, and x40 oil immersion objectives. Fluorescence images were processed using Image-Pro 6.0 software (Media Cybernetic) and Adobe Illustrator CS6 software.

4.5 Electrophysiology and *in vitro* optical imaging

Hippocampal primary cultures with transfected neurons were transferred to a recording chamber mounted on the stage of a microscope (BX50, Olympus), equipped with a water immersion x40 objective (Nikon, NA 0.8) and perfused at room temperature, oxygenated external solution (1 – 1.25 ml/min) (see below). Data were acquired using a Dagan BVC 700A patch-clamp amplifier (Dagan Corporation, Minneapolis, USA) in current-clamp mode, a 16-bit data acquisition card (National Instruments), and WinWCP software implemented by Dr. John Dempster (University of Strathclyde, UK). Patch-pipettes of borosilicate glass capillaries (GC150F-10 Harvard Apparatus) were pulled on a vertical puller (Narishige, Japan) with resistances around 7MΩ. Pipettes were filled with internal solution (~290 Osm) containing (in mM) 130 K^+-gluconate, 7 NaCl , 0.1EGTA, 0.3$MgCl_2$, 0.8 $CaCl_2$, 2 Mg-ATP, 0.5 NaGTP, 10 HEPES, and 2 EGTA (pH 7.2 adjusted with KOH 1M). The

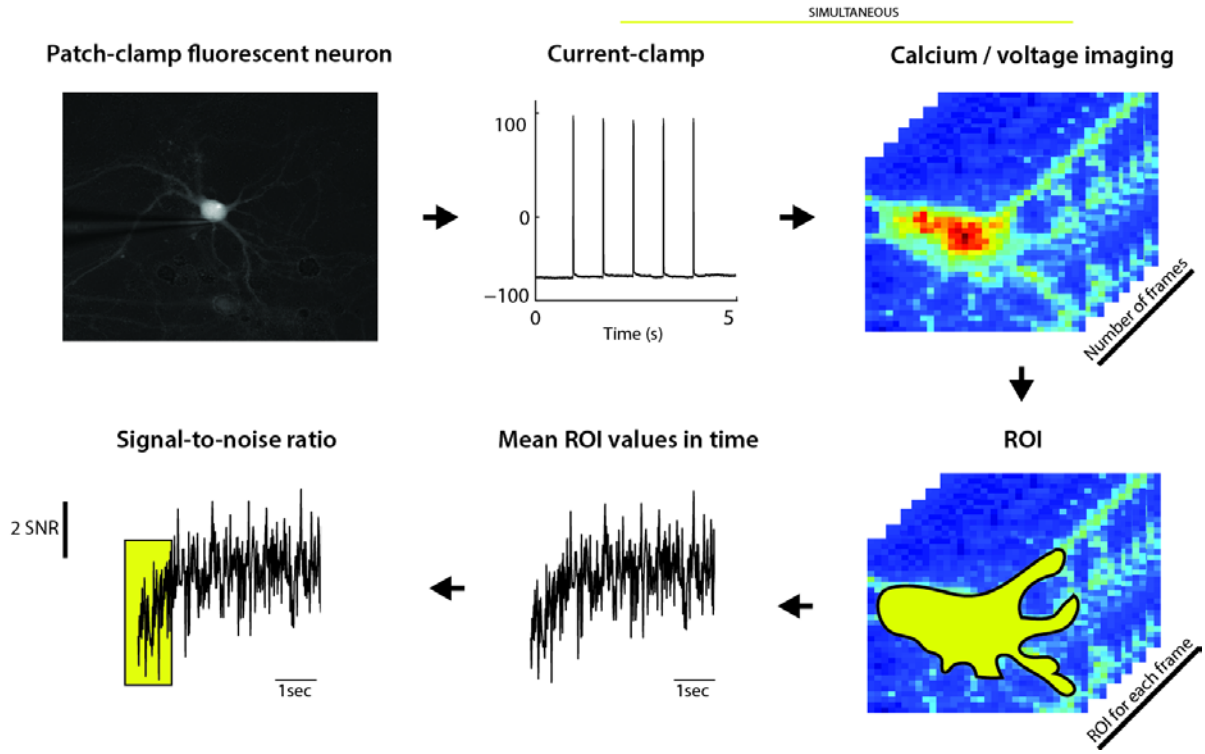

Figure 3 | Methodological scheme of data acquisition and analysis. Hippocampal cultures were transferred to a recording chamber, where current-clamp of probe-expressing neurons was performed at the same time that imaging data was acquired (they were programmed to be recorded simultaneously). Subsequently, a standard ROI was selected and one mean value was calculated from all the pixels composing the chosen ROI for each of every recorded frames. The mean values of each frame were then plotted in sequence (corresponding to the x axis – time), when SNR is measured (equation for SNR shown in Section 4.6).

external solution (~300 Osm) contained (in mM) 120 NaCl, 3 KCl, 1.2 $MgCl_2$, 2.5 $CaCl_2$, 23 $NaHCO_3$, 5 HEPES, and 11 Glucose (pH 7.4 adjusted with NaOH 1M).

APs were triggered by brief somatic current injections (2 nA, 1 ms) delivered through the patch-pipette, at frequencies ranging from 0.7 to 10 Hz. Image series were acquired using Andor DU-860 electron multiplying (EM) charge-coupled device (CCD) camera (Andor, Belfast, Ireland) and fluorescence excitation was produced by a computer-controlled 200 W metal-halide lamp (Prior Scientific). In order to lower the noise, recordings occurred under optimized settings, with a cooled CCD sensor (-80°C), dark curtains surrounding the experimental set, and slow or stopped perfusion. The number of frames was calculated for each cell; it was primarily based on the speed of the camera (~1000 frame per second), depending also on the applied exposure (time of light excitation for each cell), which varied with the baseline level of brightness in each cell.

Excitation determination was achieved selecting the bandpass filters directly at the fluorescence lamp. For exciting GCaMP3 and VSFP1.2 (Citrine excitation) we used a 480/40 nm bandpass filter; for R-GECO1excitation light passed through a 560/40 nm bandpass filter.

Emission was collected for GCaMP3 at 535/40 nm with the D535/40m filter (Chroma); for R-GECO1 (624/40 nm) and VSFP1.2 (mKate, 594 nm), HQ580/14m was used (Chroma)

In some sets of experiments, carbachol (Sigma #4382) was perfused with the external solution, at a final concentration of 10 μM, and image series were recorded without patch-clamp recordings.

4.6 Data Analysis

Data from current-clamp recordings and fluorescence were both processed and analyzed using Matlab (version 2011, Mathworks). As shown in Figure 3, for each cell at each trial, fluorescence images were recorded simultaneously to membrane voltage changes, yielding a sequence of fluorescence images (as a video) correspondent to the time course of the current-clamp protocol. For each cell, a region of interest (ROI) was selected and a mean value was calculated by the average of pixels from the selected ROI. Thereby, each image series (for each trial) was transformed from a 3 dimensional file (X *versus* Y *versus* time) into a 2 dimensional format (mean fluorescence value *versus* time). When needed, photobleaching was corrected using the 'detrend' command on Matlab. The change in fluorescence was measured by the SNR (Yamada and Mikoshiba, 2012), which was defined as the ratio of the fluorescence signal (F) to the standard deviation (SD) of *baseline fluorescence* (from immediately before the stimulus onset), where $SNR = \frac{(F-baseline)}{baseline\ SD}$. Responses were judged suprathreshold when SNR exceeded 1.

For spike detection calculations, we used the percentage of detected spikes to the total number of evoked spikes. Data analysis was performed with Matlab, ImageJ (US National Institutes of Health), and Excel (Microsoft).

4.7 Statistics

Statistical difference was assessed using independent t-student and paired samples t-test when two groups were compared or one-way ANOVA (p =0.05) followed by Tukey's when comparing more than 2 groups. Statistics was performed with IBM SPSS (version 17). Data is reported as mean ± standard error of the mean (SEM), otherwise stated.

"If a man will begin with certainties, he shall end in doubts; but if he will be content to begin with doubts he shall end in certainties"
Francis Bacon

5 RESULTS

5.1 Expression of probes in mature neuronal cultures

5.1.1 Expression of probes

The three genetically-encoded probes compared in this study were successfully expressed in hippocampal neurons, observed after 7-10 DIV (up to 35 DIV). As demonstrated in Figure 4, VSFP-expressing neurons showed distribution of the protein throughout all segments of the cells, allowing clear visualization of full processes, including dendritic spines. Intracellular agglomerations were occasionally observed in the soma, as it is revealed in Figure 4A. GCaMP3- and R-GECO1-expressing neurons also demonstrated full expression of the probes (Fig. 4B, C), with the special aspect that most of the cells had no nuclear labeling, an important indicative of the cells' health and ideal synthesis of the probe (Tian et al., 2009; Yamada & Mikoshiba, 2012).

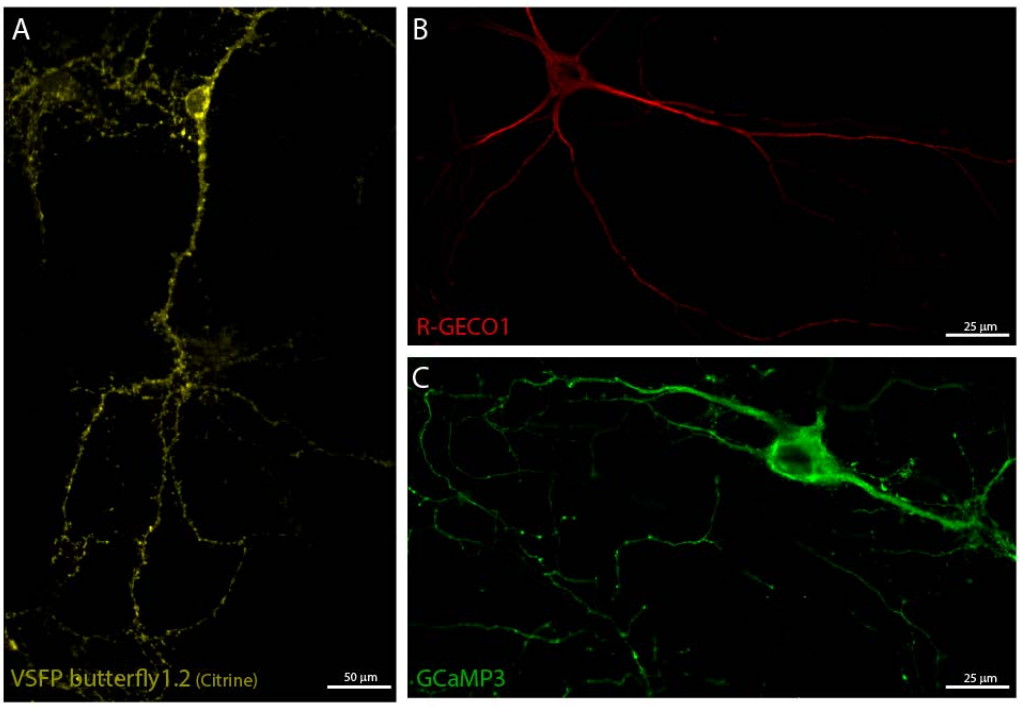

Figure 4 | Genetically-encoded probes expressed in hippocampal neurons. (A) Fluorescence image showing a VSFP butterfly1.2-expressing neuron (fluorescence only for Citrine); (B) and (C) present the neurons expressing the calcium-indicators R-GECO1 and GCaMP3 respectively, showing no nuclear expression.

5.1.2 Expression of markers for neuronal maturation

In order to ensure that cultures were sufficiently mature for patch-clamp recordings and optical imaging, we investigated the expression of two proteins that are indicative of neuronal maturation. Cultures with 13 DIV were fixed and submitted to immunocytochemistry protocols, revealing the presence of synapsin-1 and MAP-2 (Fig. 5), demonstrating the neurons to be mature (MAP-2) and functional (synapsin-1).

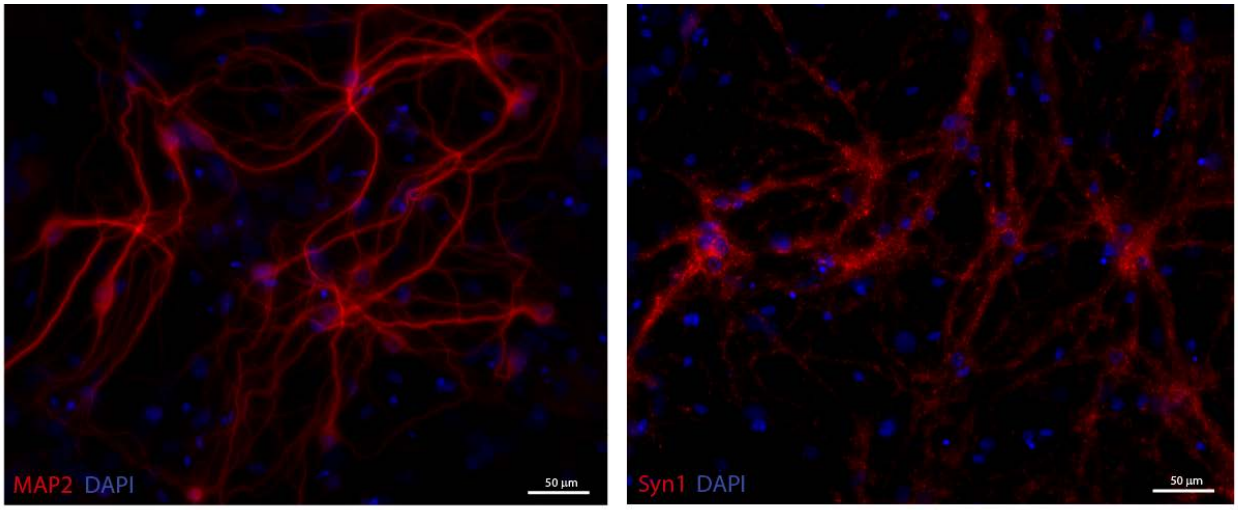

Figure 5 | Neuronal markers of maturation expressed in hippocampal neurons (13 DIV). Left figure demonstrates expression of MAP-2 in a culture of hippocampal neurons, while on the right, neurons express synapsin-1 (Syn1) and indicate the presence of synapses. In blue, DAPI marks the nuclei.

5.1.3 Electrophysiological features of neurons

Neurons were patched and their basic electrophysiological parameters were obtained. As shown on Table 1, one-way ANOVA revealed no differences among the three groups of neurons (each expressing one of the reporters) when comparing their membrane potential values (in mV): GCaMP3: -56 ±8.0, R-GECO1: -57 ±2.5, and VSFP1.2: -60 ±3.9 ($p = 0.86$). However, when the values for input resistance were evaluated, one-way ANOVA followed by Tukey's test revealed the group of neurons expressing VSFP1.2 showed a lower average when compared to GCaMP3 (in MΩ): GCaMP3: 161 ±18.3; GECO1-R: 128 ±15.3; VSFP1.2: 94 ±14.0 (GCaMP3 > VSFP1.2; $p = 0.02$). This difference found might be an indicative that the expression of VSFPs could alter neuron's fundamental constitution, as previously discussed by the original authors themselves (Mutoh, et al., 2009).

5.2 Signal-to-noise ratio

Patched neurons were submitted to current injections at different frequencies (0.7, 1, 3, 5 and 10+ Hz) and their corresponded fluorescence response was imaged. Two important

considerations were relevant to the definition of experiments: I) it has been shown that it is possible to detect individual APs with GCaMP3 at 6 Hz (Tian et al., 2009), so we wanted to compare the reporters to observe if APs at 10 Hz would be distinguishable (Fig. 6A); II) most studies performing Ca^{2+} imaging have centered their attention to signals from dendrites only (Hires et al, 2008), so we decided to compare the efficiency of the SNR from the soma and dendrites (Fig. 6B, Fig. 10).

5.2.1 Signal-to-noise ratio at 10 Hz

It is important to state that not all the neurons expressing a reporter had signal in response to the evoked APs, as shown in Table 1. In our study, only 26.7% (4/15) of the neurons expressing VSFP1.2 showed detectable fluorescence signal in response to APs. Among the GCaMP3 expressing neurons, 80% (8/10) exhibited signal, while for the R-GECO1 neurons, 50% (2/4) of the neurons had detectable signal (mean values are from the soma, if not stated otherwise).

Table 1 | Electrophysiological properties and SNR of cultured hippocampal neurons expressing different probes.

Electrophysiological property	GCaMP3 (n = 8)	R-GECO1 (n = 4)	VSFP butterfly 1.2 (n = 15)	*p*-value[a]
Resting membrane potential (mV)	-56 ± 8.0	-57 ± 2.5	-60 ± 3.9	0.86
Input resistance (MΩ)	161 ± 18.3	128 ± 15.3	94 ± 14.0	*0.02
Signal-to-noise ratio (5 APs 10Hz)	**(n = 8)**	**(n = 2)**	**(n = 4)**	***p*-value[c]**
Soma	21 ± 6.69	52 ± 19.7	1.3 ± 0.21[b]	0.25
Dendrite	14±4.0	18±3.13	-	0.52
Percentage of cells with signal	80 (8/10)	50(2/4)	26.7 (4/15)	-

[a] *Comparison included GCaMP3, R-GECO1, and VSFP butterfly 1.2 (One-way ANOVA);* [b] *The kinetics of VSFP butterfly 1.2 allows for the detection of single APs, instead of the sum of SNR seen with GCaMP3 and R-GECO1;* [c] *Comparison included only GCaMP3 and R-GECO1 (independent samples T-test);* [*] *Post-hoc analysis of Tukey's (GCaMP3 > VSFP1.2; p = 0.02).*

In order to achieve representative values for each of the three reporters and then compare their SNR means, only values from the responsive cells were considered for the SNR calculations, as represented in Table 1. The average SNR obtained from the VSFP-expressing neurons in response to five pulse injections at 10 Hz was small (1.3 ± 0.21), however the rapid kinetics of the VSFP1.2 allowed discrimination of individual APs as separated peaks. On the other hand, the calcium indicators showed the greatest changes in fluorescence following the same protocol (five APs at 10 Hz). GCaMP3 cells presented an averaged SNR value of 21 ±6.69 and R-GECO1, SNR of 52 ±19.7. One-way ANOVA

revealed no differences among the three groups (p = 0.25). Analysis of the SNR values collected from dendrites (Table 1) were collected only from the two calcium indicators and were compared with an independent samples T-test, showing no differences between the two groups (p = 0.52). Furthermore, we compared SNR scores from within the same groups, but originating from different parts of the neurons (soma *versus* dendrite). Paired samples t-test for SNR means of GCaMP3-expressing neuron yielded no differences (p = 0.23), as for R-GECO1 (p = 0.52).

5.3 Spike detection

As SNR scores detected from soma were higher (Table 1), such signals were exploited to investigate the percentage of APs detected with the three probes (cells with no evoked signal were not included). None of the reporters detected all spikes: by using VSFP1.2 (n = 4), 53% of the evoked APs were detected (Fig. 6A for individual cells; 6B for mean values). For protocols at 10 Hz, among the GCaMP3-expressing neurons (n = 8), 54% of the evoked APs were detected when selecting the soma as ROI, while with R-GECO1 (n = 2), 85%. One-way ANOVA revealed no differences for the percentage of detected APs through the signal from the soma (p = 0.256). Also, we compared signals collected from dendrites (not from VSFP1.2) with independent samples T-test, showing no differences: GCaMP3 62.2% (n = 6) and R-GECO1 100% (n = 2) (p = 0.136).

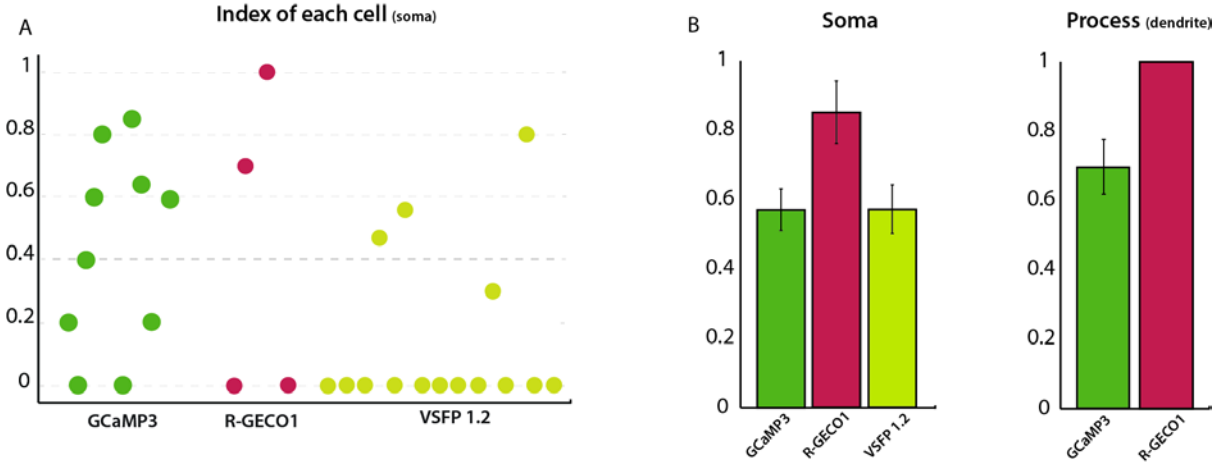

Figure 6 | Index of spike detection rates using GCaMP3, R-GECO1, and VSFP butterfly1.2. Neurons were submitted to spike trains at 10 Hz with simultaneous imaging. Indexes were calculated as the number of detected spikes divided by the total number of spikes induced (range: 0.0 – 1.0). (A) Scatter plot for individual cells' indexes highlights that only the minority of the VSFP-expressing neurons exhibited detectable fluorescence signal in response to the evoked spikes 26.7% (4/15); for GCaMP3, 80% (8/10) of the neurons exhibited signal, while for the R-GECO1, 50% (2/4). (B) Average index of spikes detected includes only cells exhibiting evoked fluorescence response. ROI from the soma (left) demonstrates that signals from VSFP1.2 neurons (n = 4) detect ed53% of the evoked APs; from GCaMP3-expressing neurons (n = 8), 54%, and R-GECO1 neurons (n = 2), 85%. ROI collected from dendrites (right), signals from GCaMP3 neurons (n = 6) discriminated 62.2% of the spikes and R-GECO1 (n = 2) neurons, 100%.

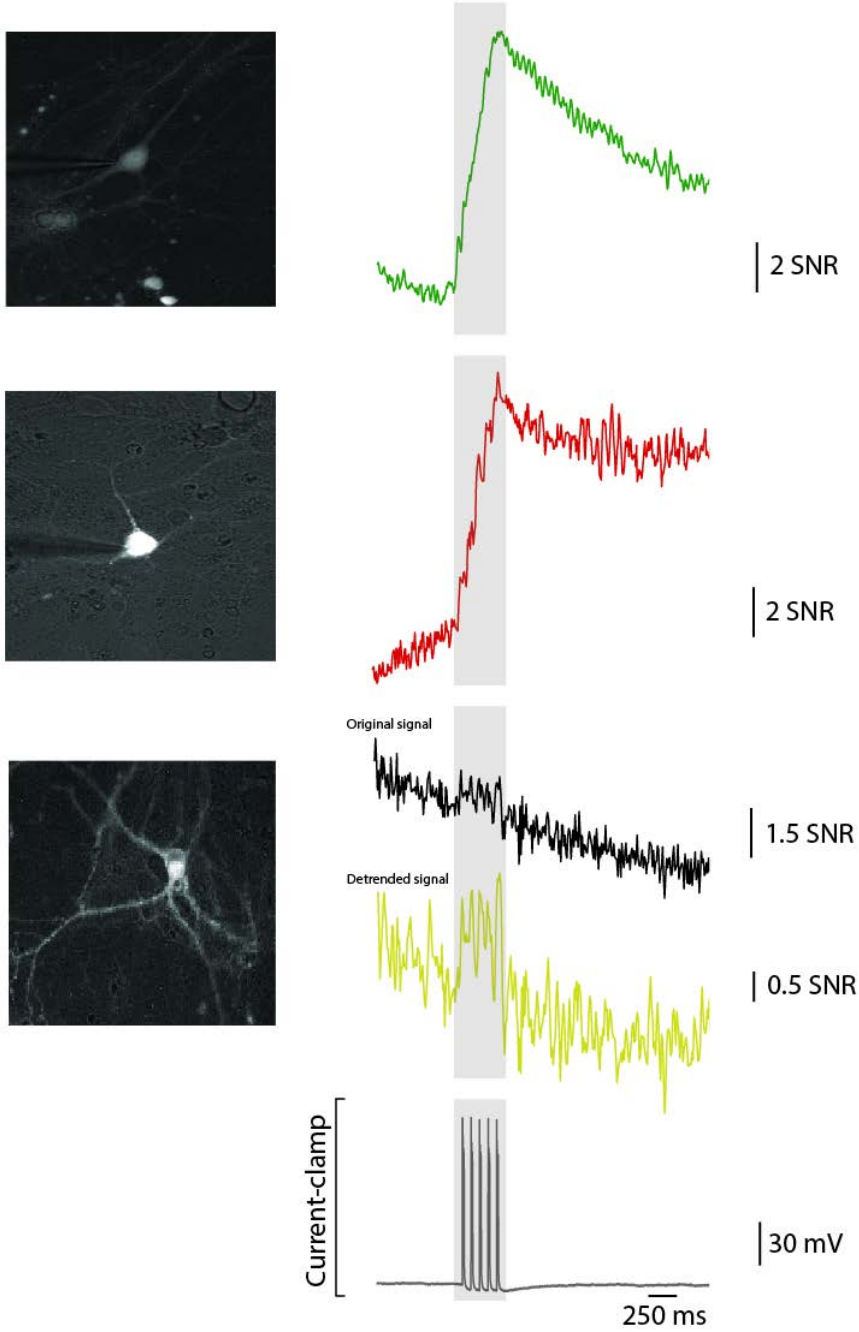

Figure 7 | Fluorescence signals from individual neurons in response to 5 APs at 10 Hz. On top, it shows a patched GCaMP3-expressing neuron and its calcium response, reaching a SNR of ~20, similarly to the R-GECO1-expressing neuron (in the center), showing also a signal of ~ 20SNR. At the bottom, VSFP-expressing neuron shows discrete fluorescence signal (~1 SNR) evoked by the 10 Hz spike train (current-clamp represented as well). Although the rapid kinetics of the VSFP allowed discrimination of individual APs as separated peaks, signals from VSFP did not show accuracy and noise could be confused with AP peaks.

As demonstrated in Figure 7, unless combined with current-clamp recordings, signals from VSFP1.2 do not show sufficient accuracy, so that in certain segments where no spikes occurred, the high noise could be confused with AP peaks (Fig. 7). Furthermore, frequencies below 5 Hz and subthreshold signals were not discernible using VSFP1.2, also due to high noise (data not shown). With the calcium-indicators, on the other hand, APs were evidently detectable in all the analyzed frequencies, as well as subthreshold depolarizations (Fig. 7, Fig. 8).

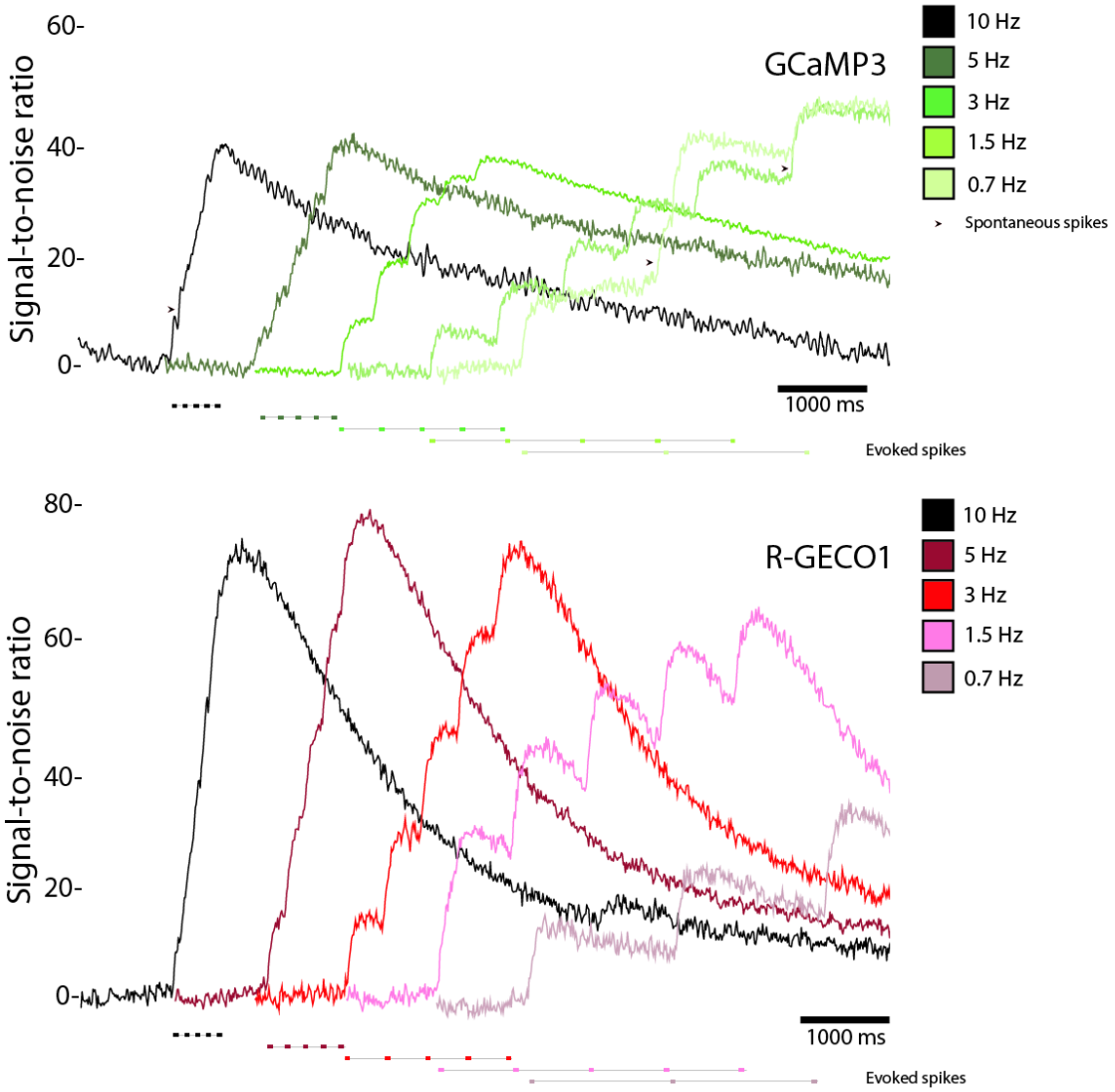

Figure 8 | Calcium imaging and current-clamp at different frequencies. SNR values from single neurons in response to five APs induced at 10, 5, 3, 1.5, and 0.7 Hz (single trials) and clear discrimination of evoked APs at the different frequencies. Arrows on the GCaMP3 figure indicates spontaneous spikes detected by current-clamp recording.

5.4 Applications of GECIs

Our results demonstrated that GCaMP3 and R-GECO1 showed no impairments to the expressing neurons (Table 1) and constituted the groups that most likely yielded fluorescence responses and with higher SNR values (Fig. 6, Fig. 7). Given the aforementioned encountered characteristics, the following experiments were performed only with the two calcium-indicators.

5.5 Spatial discrimination

In Figure 9, we show that GCaMP3 is an efficient indicator of neuronal activity, possessing good spatial and temporal resolutions, capable of discriminating the origin of synaptic inputs at different processes of the same neuron. As seen in Figure 9C, we show four cells recorder (Fig. 9D) with a clear demonstration of the activation of only one of the cells with high spatial and temporal discrimination (Fig. 9C). Furthermore, in Figure 9A, we show a patched neuron submitted to five pulse injections at 10 Hz with simultaneous calcium imaging. As demonstrated in Figure 9B, by selecting ROI from defined segments of the same neuron (Fig. 9A; soma and two different processes), subcompartmental resolution was achieved and we were able to infer the origin of an EPSP that had firstly been detected with the current-clamp.

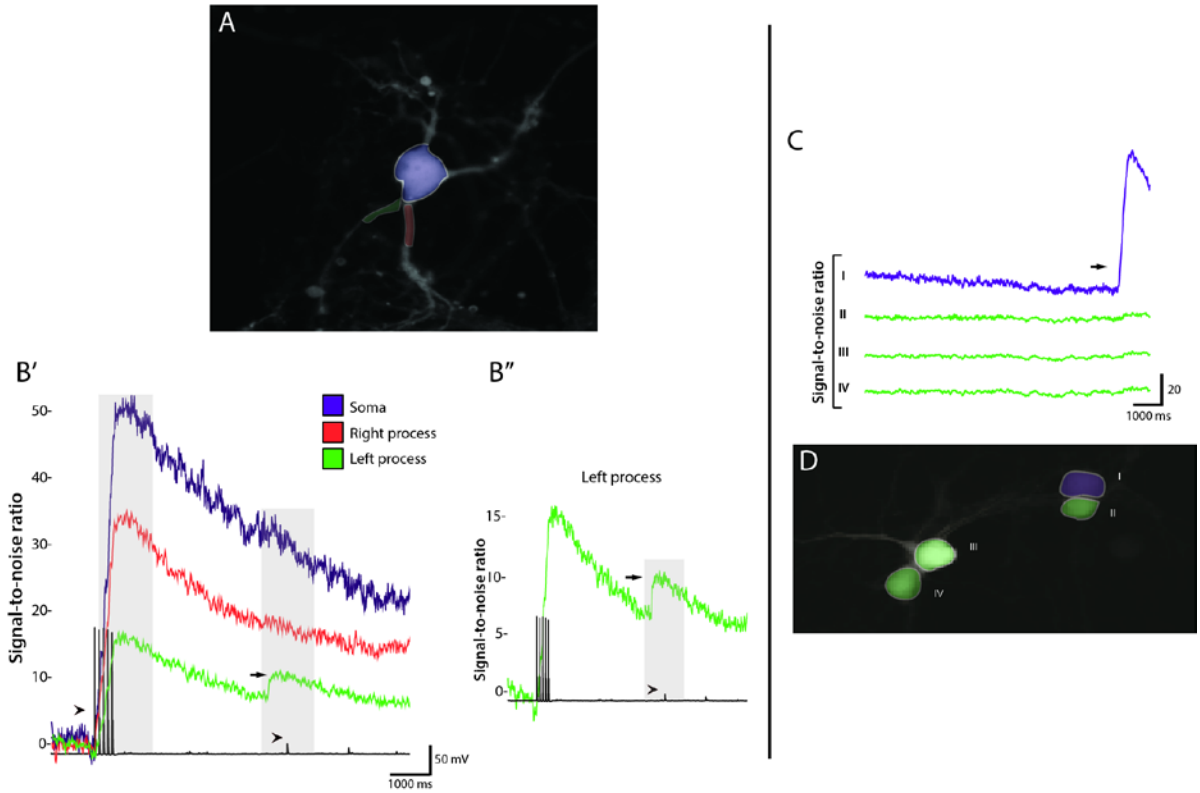

Figure 9 | Reliable spatial discrimination achieved with GCaMP3. (A) Patched neuron expressing GCaMP3 with ROI for the soma labeled in purple and ROI for two different processes in green and orange. (B') Current-clamp (5 APs at 10 Hz) and SNR from defined segments of the same neuron demonstrates the origin of an EPSP firstly detected with the soma current-clamp; (B'') showing the arrival of the EPSP at the specific process (in green). (C, D) Simultaneous imaging of four neurons clearly demonstrates that the GCaMP3 allows the discrimination of the activated or silent cells with high spatial and temporal resolutions.

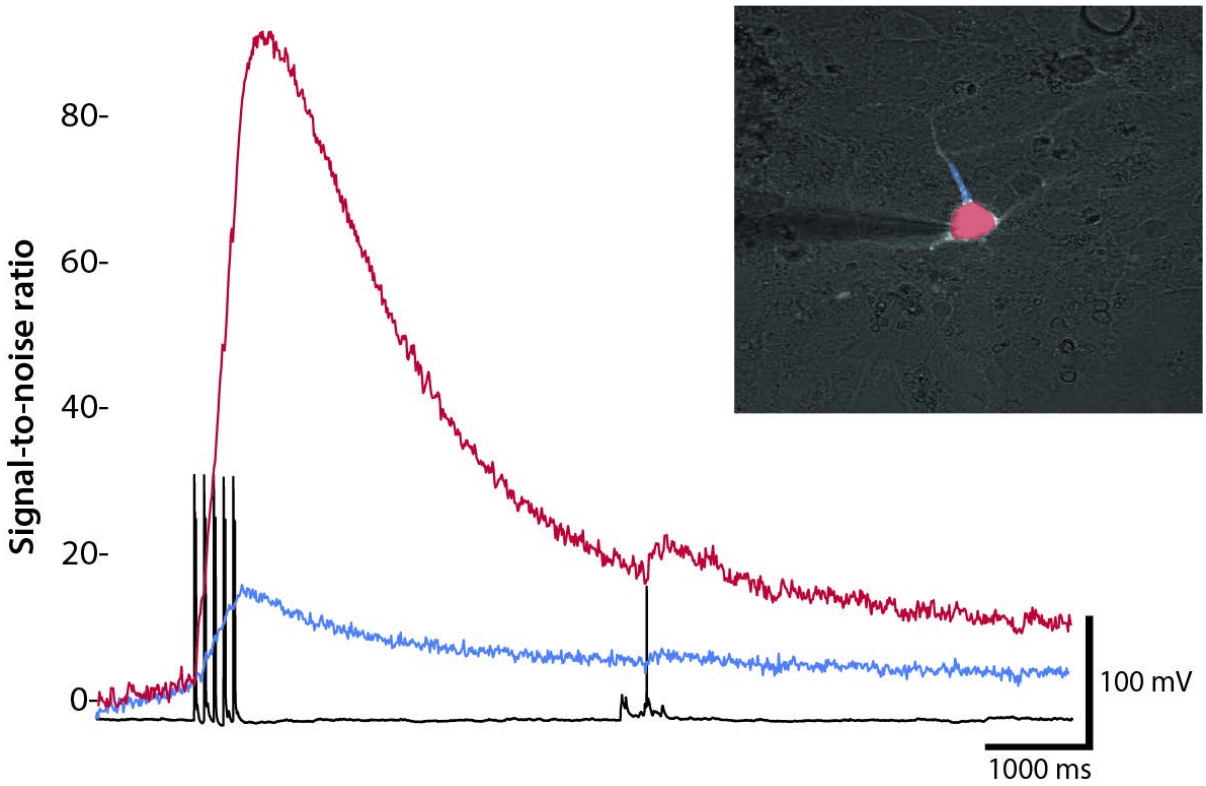

Figure 10 | Detection of spontaneous AP from R-GECO1-expressing neuron. Current-clamp of R-GECO1-expressing neuron exhibits a spontaneous AP that was confirmed with calcium imaging from the soma. Apparently consisting of a situation in which EPSPs arrived at the neuronal soma (in red), since no Ca^{2+} response was detected at the investigated process (in blue).

The study of Ca^{2+} dynamics requires the consideration of the highly distinct nature of Ca^{2+} events in response to APs evoked by artificial current injections (antidromic) and those spontaneously occurring due to a summation of synaptic inputs. In that regard, whereas evoked APs trigger mainly the opening of voltage-sensitive calcium-channels (VSCC), Ca^{2+} influx coming from synaptic inputs can be originated from a variety of different sources, such as NMDA receptors, subtypes of AMPA receptors, internal storages, and VSCC as well (Higley & Sabatini BL, 2008). When studying calcium events in neurons, naturally occurring spikes also permit the monitoring of synaptic activity itself, such as the 'when' and 'where' of arriving EPSPs, with interesting and potentially different events.

As demonstrated in Figure 9B, current-clamp recording from the soma of a GCaMP3-expressing neuron showed a subthreshold membrane depolarization. Calcium imaging with GCaMP3 made possible not only its confirmation (with temporal resolution), but also to prove from which dendritic process the synaptic input had reached the patched neuron. Likewise, patch-clamp recordings of a R-GECO1-expressing neuron revealed a spontaneous AP and we compared the calcium signal collected from the soma to the signal from one process (Fig. 10). In this particular case, we believe that it represents a situation where EPSPs

arrived directly at the neuronal soma, for the absent Ca^{2+} response at the dendrite but prominent signal from the soma triggering an AP

5.6 Antidromic spikes *versus* spontaneous activity

The range of questions that can be addressed with the usage of GECIs is wide. Nevertheless, important complications arise from the fact that Ca^{2+} influx resulting from evoked APs and synaptic activity fluctuates in vast amplitudes, depending on the number and property of the synapses recruited, on the type of the neuron involved, and on temporal aspects regarding calcium buffering and extrusion (Scheuss et al., 2006). When using GECIs, the goal is the faithful and accurate measurement of calcium events without the need for patch-clamp recording. Thus, discerning between EPSP and actual spikes is crucial.

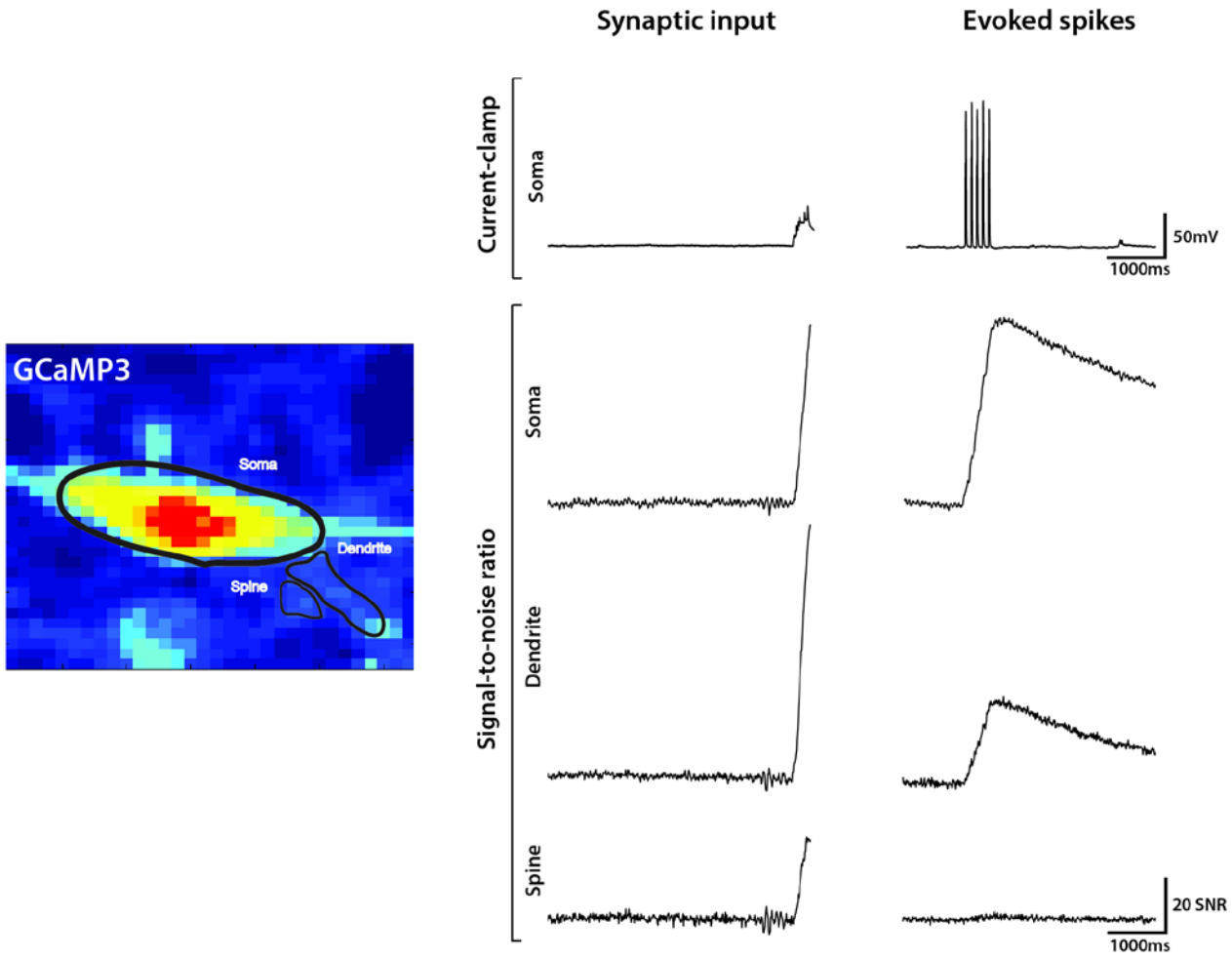

Figure 11| Evoked APs *versus* naturally occurring EPSPs/APs. Patched GCaMP3-expressing neuron under two conditions; on the left, spontaneous EPSP led to a ~30 mV change at the membrane potential resulting in ~ 70 SNR from the soma, 110 SNR from the dendrite, and 30 SNR from the spine. In the second condition, calcium imaging of a 5AP-train rendered smaller signals: soma signals were similar to the EPSP (~70 SNR); however, dendritic signals reached less than 30 SNR, with basically no detectable SNR from the spine.

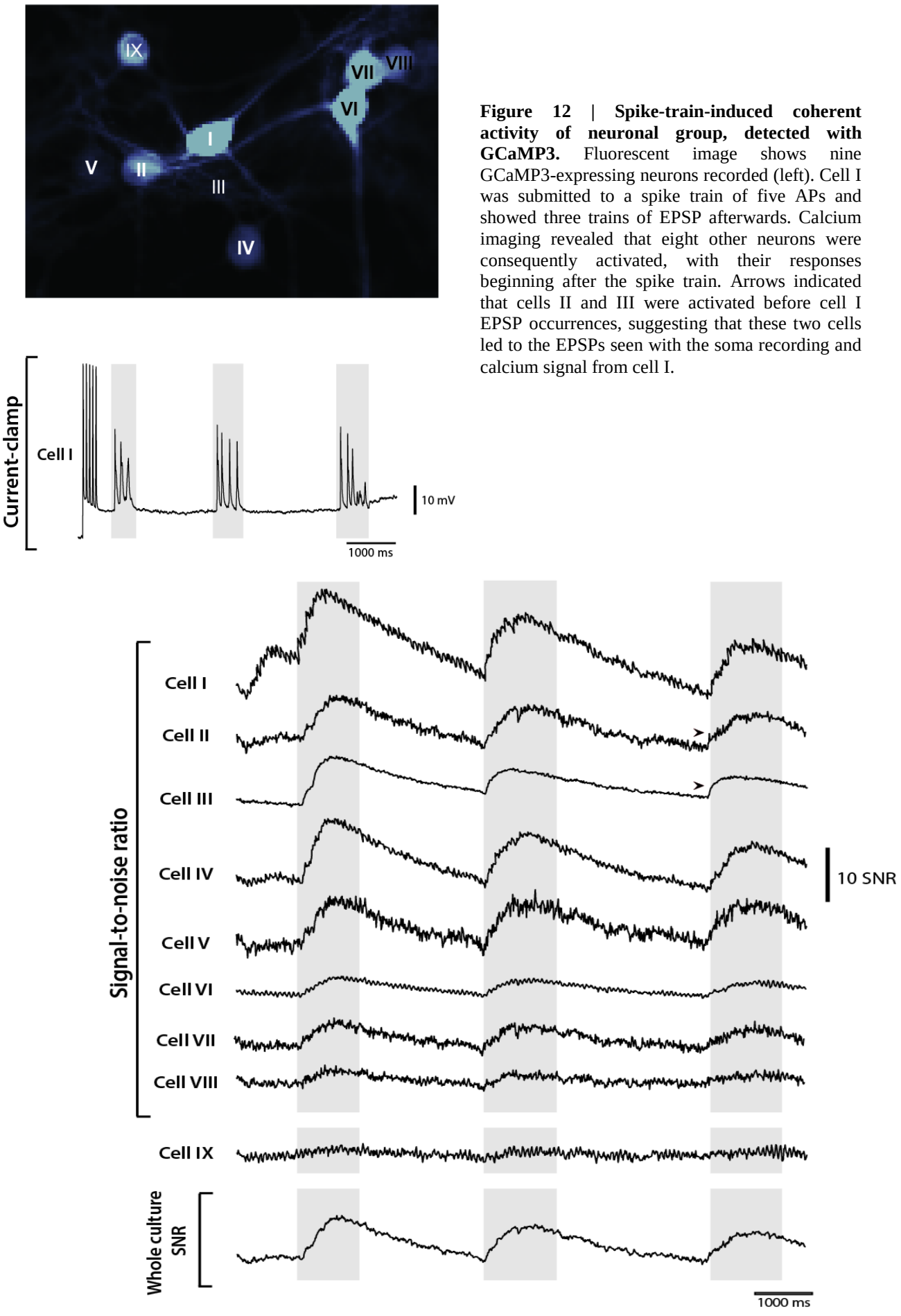

Figure 12 | Spike-train-induced coherent activity of neuronal group, detected with GCaMP3. Fluorescent image shows nine GCaMP3-expressing neurons recorded (left). Cell I was submitted to a spike train of five APs and showed three trains of EPSP afterwards. Calcium imaging revealed that eight other neurons were consequently activated, with their responses beginning after the spike train. Arrows indicated that cells II and III were activated before cell I EPSP occurrences, suggesting that these two cells led to the EPSPs seen with the soma recording and calcium signal from cell I.

In that perspective, our results bring preliminary insights on ratiometrics' difficulties related to this subject. In Figure 11, we show SNR values from a GCaMP3-expressing neuron in two conditions: I) spontaneous EPSP leading to ~30 mV change (at the membrane potential) and II) five evoked APs at 10 Hz. Calcium imaging was measured from different segments of the cell for both conditions. When selecting a ROI from the soma, calcium signals from both cases had the same amplitude (~ 70 SNR), although with very different membrane depolarizations and, above all, different physiological meanings. Interestingly, when comparing the ROI from the dendrites, the amplitude of the signal reached up to 110 SNR from the EPSP condition, while the antidromic spikes yielded not more than 35 SNR. Selecting a ROI from a dendritic branch (or spine), we found another striking difference in signal, with no signal being detected after the induced APs, but a value higher than 30 SNR from the synaptic inputs.

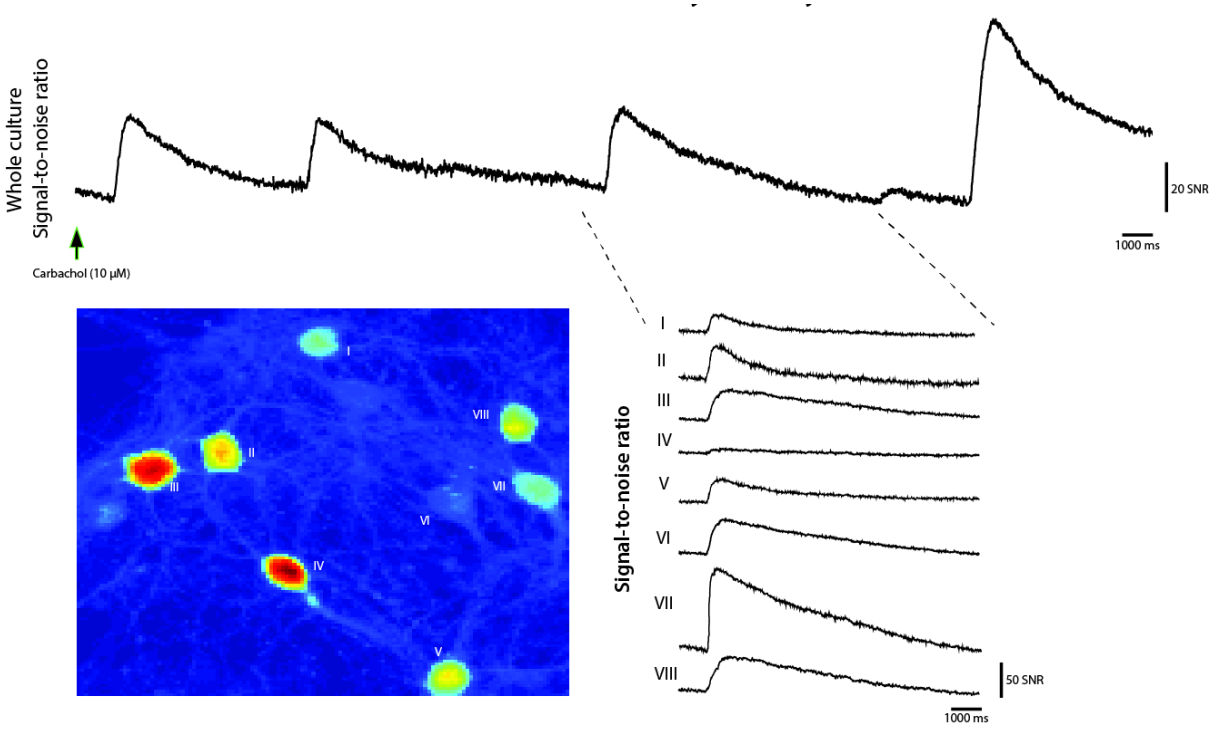

Figure 13 | GCaMP3 detection of carbachol-induced synchronic activity of cultured neurons. Application of carbachol (10 µM) drove cultured hippocampal neurons to coherent activity. Calcium imaging of eight individual cells, as well as when considering all cells together, demonstrated synchronous SNR values.

5.7 Synchronization

One of the greatest advances of using genetically-encoded activity indicators is the possibility to monitor groups of neurons with high spatial and temporal resolution. Therefore, this approach is especially useful to study connectivity and synchronous activity in defined neuronal networks.

In calcium imaging of groups of cells, GCaMP3 showed clear discrimination between activated and silent cells, also permitting visualization of synchronous activity of up to 8 cells. In Figure 12, one patched cell (cell I) was submitted to a spike train that induced five APs. From the current-clamp recording, it was seen that, after the evoked spikes, the neuron received sequential EPSPs that resulted in trains of spikelets. With calcium imaging of the neurons surrounding the patched neuron, we found that seven other cells were now simultaneously activated, with their calcium signals (responses) initiating after the induced spike train. Moreover, not all the viewed cells displayed activity, revealing GCaMP3 as an accurate indicator to distinguish active from silent cells. When the signal from the whole group of neurons was considered, the sum of the activity of the eight cells indicated that a synchronic event took place, visualized by the clear matching of the SNR temporal patterns collected from the studied cultured neurons. Moreover, we also showed that cells II and III have spiked before cell I on the third spikelet-train (shown with arrows), suggesting that from these two cells resulted the EPSPs seen by the soma recording and calcium signal from cell I.

Finally, we applied carbachol to a hippocampal culture of GCaMP3-expressing neurons, because this pharmacological treatment is known to induce neuronal synchronization in a wide range of *in vitro* and *in vivo* preparations (Bianchi & Wong, 1994). In Figure 13, with calcium imaging of single-cells and from the whole culture, we demonstrate high SNR values from the neurons, in a coherent manner, suggesting a successful induction of synchronized activity. As expected by the action of carbachol on the acetylcholine receptors, SNR values were much higher probably due to the massive calcium influx from the activated receptors.

"Our image of the nerve cells […] is like a collage of many overlapping views, patiently accrued during a century of study."
Alan Peters, 1991

6 DISCUSSION

In the present study, we tested the performance of three of the latest genetically-encoded indicators in cultured primary hippocampal neurons: the calcium-indicators GCaMP3 and R-GECO1, and the voltage-indicator VSFP1.2. Under our particular expression and imaging conditions, our findings suggest that (1) VSFP1.2 might disturb the physiology of neurons, due to the lower input resistance found in this group of neurons; (2) GCaMP3 exhibited the highest percentage of neurons showing fluorescence readouts in response to evoked spike trains; (3) GCaMP3 and R-GECO1 are apparently more suitable for detecting APs at frequencies up to 5 Hz, although the fluorescence from some VSFP1.2-expressing cells were correlated to APs at 10 Hz as individual peaks; (4) GECIs were shown to be reliable tools for investigations on calcium dynamics with good spatial and temporal resolution for individual or multiple neurons simultaneously; (5) finally, we compared GECI fluorescence readouts from evoked APs *versus* spontaneous APs and EPSPs, showing that membrane depolarization amplitudes do not necessarily evoke a linear calcium response, varying with sum of synaptic inputs reaching the neurons.

GEVIs and GECIs comprise different advantages/disadvantages and, up to date, this is the first study comparing the two major classes of neuronal activity reporters, under similar experimental setups. The decision to compare these specific probes was based on different parameters founds in each of the probes, including not only a wide dynamic range and fast kinetics, but also the light spectrum they cover. Regarding the choice to use of GCaMP3, it shows brighter readouts, greater protein stability, and larger dynamic range compared to previous versions, besides being the most extensively employed GECI (Tian et al., 2009; Yamada et al., 2011; Zhao et al., 2001; Yamada & Mikoshiba, 2012). However, it is broadly acknowledged that optical imaging of neurons expressing FPs requires high intensity excitation, which leads to the massive production of reactive oxygen species (ROS), causing photo-oxidative damage to the cells (Wright et al., 2002). By reacting with proteins, lipids, and nucleic acids (Halliwell and Gutteridge, 1989), the increase in ROS can alter the physiology of neurons, determining significant cell damage. If cells are exposed to low levels

of irradiation, the production of ROS is known to be reversible (Dixit and Cyr, 2003) and the cell conditions are maintained ideal. Nevertheless, not every experimental design can be addressed with short exposure times, and long-term *in vivo* experiments in which the same neurons are recorded numerous times can present a problem.

In that sense, an alternative is the use of red-shifted FPs, such as the R-GECO1 and the VSFP Butterfly 1.2. Red-shifted fluorescent indicators constitute better alternatives compared to blue-shifted ones because of the lower energy and consequently smaller phototoxicity (Dixit and Cyr, 2003). Besides, they possess a crucial benefit for *in vivo* experiments: longer wavelengths have deeper tissue penetration, so that light can be delivered to deeper brain areas, broadening volume of brain tissue that can be investigated (Zhang et al., 2008). Moreover, it has been shown that autofluorescence and absorption of light by tissues are decreased in the red compared with the blue and green segments of the visible light spectrum (Kremers et al., 2011).

The choice of employing R-GECO1 implies important positive features. Being developed from the framework of GCaMP3, essentially all the biophysical and calcium-sensitivity features of GCaMP3 remained unaltered on R-GECO1 (Zhao et al., 2011) and, furthermore, the presence of mApple as its FP reduces photodamage when compared to GCaMP3 that has GFP as its FP. Because of their non-overlapping light spectra, the possibility to use both GECIs under the control of different promoters makes it possible to evaluate calcium dynamics of different neuronal populations concomitantly. However, even though it represents an option to overcome the phototoxicty of traditional blue/green-reporters, it has already been shown that the emission of mApple is blue-shifted to some extent (~18nm), which must be considered when using multiple FPs, in order to avoid spectral overlaps with yellow and orange FPs (Shcherbo et al., 2009).

When choosing the best variant of VSFP, the broad palette contains different versions covering from blue to far-red light spectra and possessing variable kinetics and efficacy on membrane expression (Knöpfel et al., 2010; Mutoh et al., 2009). The recently released VSFP1.2 possesses the best kinetics and has been able to detect APs *in vivo* (Akemann et al., 2012). And because it contains the far-red mKate2, it also represents an option to reduce cell the damage associated phototoxicity. On the other hand, even though it is considered the version with the best membrane targeting, the use of mKate in other contexts has been

associated with intracellular aggregations (Kremers et al., 2011), in accordance to what we have seen in a portion of our cells (Fig. 7).

6.1 Phenotype of neurons

We have shown that neurons expressing each of the reporters were sufficiently mature after two weeks in cultures (for up to 35 days), confirmed by the expression of MAP-2 and synapsin-1 (Fig. 5), as well as resting membrane potentials of the three groups around -60 mV (Table 1) and full APs were evoked from all the neurons included in this study. Concerning the expression of the probes (Fig. 6 and 7), their distribution corresponded to the expected pattern encountered in previous studies and comprised the full neuronal extension: both calcium indicators were located in the cytoplasm, while the VSFP1.2 had its main expression on the membrane.

Although expressing genetically-encoded indicators is minimally invasive when compared to dyes, a variety of cellular perturbations, such as calcium buffering and protein interactions can occur. In that regard, in our study the expression of the GECIs was delimited to the cytoplasm, reaching the full length of the neurons (Fig. 4). Interestingly, however, the original study characterizing R-GECO1 did not show images of expressing-neurons (Zhao et al., 2011); the first group to employ this probe demonstrated its expression invading the nucleus, along with cytoplasmic agglomerations of the protein (Yamada & Mikoshiba, 2012). In our neurons, on the other hand, there was no nuclear labeling and the expression was confined to the cytoplasm (Fig. 4B), a crucial indicative of the cells' health and ideal synthesis of the probe (Tian et al., 2009). Moreover, no electrophysiological or structural impairments were observed.

Still in that sense, studies using GCaMP3 have shown that the pattern of expression in some cells included not only the cytoplasm, but also the nucleus of the neurons, which was associated to impaired calcium homeostasis and function of GCaMP3 (Tian et al., 2009). In such cells, it has been argued that perhaps due to excessive expression, there would be misfolding and protein interactions, leading to invasion of the nucleus – associated with loss of GCaMP3 functionality and lack of response to changes in [Ca^{2+}]. In our experiments, we opted to not choose such cells for our patch-clamp experiments. However, we have included such atypical cells when imaging from groups of cells and surprisingly, we have observed that they are responsive (Fig. 13; cells III and IV), reacting similarly to cells with the ideal cytoplasmic expression.

A possible explanation for these nonfunctional indicators could be that GECIs composed by CaM (such as the GCaMP3 and R-GECO1) could be sequestered by proteins involved with endogenous calcium-signaling cascades (Palmer and Tsien 2006). Furthermore, when highly expressed, GECIs can impair or modify their natural calcium signaling and potentially act as dominant calcium buffers, altering duration, amplitude, and spread of calcium transients depending on the subtype of neuron. Early studies employing the GCaMP2, a previous version of GCaMP3, showed attenuated responses to AP trains in neurons from cortical slices (Hires et al., 2008), while others have also expressed GCaMP2 in cortical cells for up to 4 weeks and did not observe any interference with cells' health (Mao et al., 2008). With respect to *in vivo* experiments, behavioral impairments have been seen with the expression of GCaMP2 in *Caenorhabditis elegans* (Tian et al., 2009), proving the importance of reliable evaluations of new indicators. This interference could be alternatively reduced with reporters based on calcium-binding proteins not originally found in neurons, such as the troponinC-containing GECIs, e.g. TN-XXL (Mank et al., 2008).

Cellular perturbations are also likely to occur with the expression of the transmembranic VSFPs, although such aspects have been less addressed. Under our experimental conditions, when the values for input resistance were evaluated, the lower values found on the VSFP-expressing neurons might be an indicative that its expression could alter the neurons' fundamental constitution (Mutoh, et al., 2010). The input resistance of a neuron reflects both the cell size (the smaller the cell, the higher the resistance) and the extent to which membrane channels are open at resting, with a low resistance implying higher density of open channels (high conductance). Although expressing neurons were electrophysiologically healthy, as indicated by their ability to generate evoked action potentials, lower input resistance values might suggest some stage of immaturity (Fukuda et al., 2003) or perhaps interference with other transmembrane proteins (just as ion channels). In that regard, the expression of an exogenous protein (such as VSFPs) forces the recruitment of the cell machinery on a new, diverse manner, contributing to a possible differential synthesis and transportation of proteins to the cell surface, as an adaptation to the disturbed intracellular milieu.

On the case of VSFP1.2, it contains the mKate2 as one of its FPs, which consists of a coelenterate-derived protein that has been shown to form intracellular aggregates and disturb protein trafficking within mammalian cells (Kremers et al., 2011). Even though the new

version of VSFP shows significantly better membrane targeting (Akemann, et al., 2012), intracellular agglomerations were occasionally observed in the soma (Fig. 4) and we believe that its retention within intracellular membranes or its influence on other membrane-located proteins might occur and play a role in the electrophysiological differences seen in our experimental circumstances. Moreover, even though optimization of promoters and regulatory sequences can be applied to boost up expression levels of these indicators, excessive expression can increase background noise, as well as render cellular perturbations and disrupt their feasibility. The ideal GEVI should possess higher SNR with minimal influence on endogenous intracellular proteins.

6.2 Fluorescence readouts and Spike detection

In our study, optical imaging did not always yield fluorescence readouts in response to the stimulus protocols applied (Table 1). The number of neurons expressing R-GECO1 was small (n = 4), of which 50% of the cells exhibited detectable fluorescence signal. For the other two proteins, the sampling of each group was more representative. From only 25% of the neurons expressing VSFP1.2 we could obtain fluorescence signal (n = 4/15), while 80% of the GCaMP3-expressing neurons (n = 8/10) presented detectable fluorescent emission. Surprisingly, the lack of response from VSFP-expressing neurons has never been documented (or mentioned) on previous studies. On the contrary, studies using GCaMPs variants have stated that not all the cells necessarily exhibit evoked responses (Mao et al., 2008; Tian et al., 2009).

Using the method of nucleofection, we have achieved high density of neurons expressing VSFP1.2, with reasonably dim baseline brightness – consistent with other studies (Akemann et al., 2012). The extremely low SNR evoked from the VSFPs (~1.5 SNR) has also been extensively shown (Knöpfel et al., 2010; Akemann et al., 2010; Akemann et al., 2012) and constitutes a limiting feature of this class of reporters. Here, we have shown that the few cells which exhibited SNR values similar to those previously documented (Akemann et al., 2012) displayed good kinetics, with signals presented as isolated peaks for each AP at 10 Hz (Fig. 7). The latter property of voltage-indicators represents one of the greatest advantages over indicators responding to calcium, because the more rapid kinetics of GEVIs can both perceive sparse APs, as well as (ideally) distinguish individual spikes at higher frequencies. Nevertheless, it was intriguing that less than one third of the cells showed detectable SNR evoked by APs (Table 1; Fig. 6).

First of all, as mentioned before, VSFP might not be fully functional either by misfolding or by interacting with endogenous proteins (see bellow considerations regarding FRET). Secondly, the level of expression of the probe might also play a relevant role. In that sense, no distinguishable differences could be perceived from responsive to non-responsive cells (regarding levels of expression). In order to indicate more accurate quantifications for a potential correlation between low expression and impaired performance with poor SNR, post-hoc techniques, such as immunocytochemistry could be employed. An important aspect related to the VSFPs is that their fluorescence readouts come from a FRET-based pair of FPs. An alternative option to estimate the concentration of the VSFP relies on the emission of the directly excited acceptor FP. It has been proposed that such measurement is theoretically insensitive to voltage variations, so that measuring its emission would be an indicative of levels of expression (Miyawaki and Tsien 2000). Still on the FRET phenomenon, its efficiency (i.e., the transfer of energy from a donor to an acceptor fluorophore) is inversely proportional to the sixth power of the distance linking the two FPs, making FRET particularly sensitive to small distances (Harris, D.C, 2010). Therefore, the lack of signal encountered in the majority of our imaged neurons could be due to even the smallest disturbances on the distance between the two FPs, leading to lower or undetectable emitted signals.

When comparing the expression of GEVI *versus* GECI, it is crucial to consider that voltage-sensitive probes are found in the membrane and that their full content will be corresponding to the surface of the cell (comprising the plasmic membrane). Conversely, calcium-sensitive reporters are found within the whole extent of the cytoplasm, having its expression comprising the total *volume* of the cell. Therefore, such differences in the expression patterns of GEVIs and GECIs are likely to influence the disparity observed between the dynamic ranges of members from both classes: minute SNR values for GEVIs (~1.5), opposed to high values for GECIs (>10), as found in our report, as well as in a variety of other studies (Knöpfel T., 2012).

Sparse APs trigger brief, independent calcium transients. On the other hand, APs occurring at high frequencies determine closely spaced calcium transients that will be spatially and temporally summed, so that GECIs' signals are often shown as a curve or slope, whose amplitude is dependent on (but not necessarily linear to) the number of APs involved. Because of the slow kinetics of calcium dynamics itself (when compared to membrane voltage variations), the relationship between spike-trains and fluorescence readouts must be

correlated in order to be meaningful. Therefore, differently from GEVIs, which yield individual peaks for every AP, it is a major goal to have SNR values from GECIs that are consistently linear and correlated to the number of APs involved.

According to the kinetics of GCaMP3, it has been possible to distinguish APs with GCaMP3 at 6 Hz (Tian et al., 2009), confirmed by our readouts from evoked spikes at 5 Hz (and partially at 10 Hz) seen in Figure 8. In the study in which GCaMP3 was first exploited, a screen for the linearity of the fluorescence readouts was performed: the stimulus protocol consisted of comparing different trains of APs at 83Hz (from 1 to 40 APs). In this report, the SNR responses were shown to be linear to the number of APs from 3 up to 20 APs *in vitro* (Tian et al., 2009). However, this linearity firstly encountered does not seem to be consistent to every neuronal type. In figure 8, for example, although it constitutes a case of one neuron, single APs could be separately detected at the different frequencies but the SNR values varied from ~5 to up to ~12 (in the same particular cell). In another study in which pyramidal hippocampal cells were compared with Purkinje cells, the performance of GCaMP3 was also not linear in the cerebellar neurons (Yamada et al., 2011). In that perspective, higher endogenous Ca^{2+} buffering in Purkinje cells (Maeda et al., 1999) might alter the performance of GECIs, since most have been standardized in pyramidal cells. Also, depending on the experimental setup, experiments held at higher temperatures (near physiological values) are likely to make Ca^{2+} transients faster and smaller, probably involving more active Ca^{2+} extrusion mechanisms (Markram et al.,1995). This highlights the need for more studies comparing genetically-encoded probes under similar situations and involving a variety of cell types.

Although SNR from calcium-reporters are usually sufficiently large to be detected, a major quest has been run on the development of a GECI capable of detecting single spikes, preferably *in vivo*. One attempt for detecting individual APs was based on the fact that the highest changes in $[Ca^{2+}]$ take place near the membrane (Jaffe et al., 1992). Therefore, these authors targeted GCaMP2 to the plasmic membrane in the effort to make the readouts from calcium transients more efficient; however, no improvements were found (Mao et al., 2008). As aforementioned, for the standardization of the GCaMP3, SNR responses were detectable from 3 up to 20 APs (Tian et al., 2009), with unsatisfactory responses for individual spikes.

An improved YC variant, D3cpVenus, has been reported to detect single APs in pyramidal neurons in mouse cortical slices and *in vivo* (Wallace et al., 2008), but its slow

kinetics has hampered its applicability. In a study comparing different versions of YC and the GCaMP3, Yamada and collaborators (2011) show that the YCs exhibit detectable SNR for 1AP *in vitro*, but GCaMP3 does not (although in some of our cells GCaMP3 and R-GECO1 were successful). The new family of GCaMPs, named the GCaMP5s, includes a variant that enables the detection of single spikes (*in vitro*), possessing in addition the other benefits of the state-of-the art GCaMPs: increased fluorescence baseline and dynamic range, great photostability, and fast kinetics (Akerboom et al., 2012).

The rapid development and widespread usage of fluorescent probes demanded the creation and optimization of fluorescent microscopy techniques (Peixoto et al., in preparation). Nowadays, improvements in order to optimize the use of VSFPs can be employed, such as faster cameras (with larger number of frames per second), more specific filters for the FPs, and the 60x water immersion objectives, which have larger numerical apertures to minimize bleaching and virtually detecting every photon reaching the sensor (here we used a 40x). Concerning limitations of calcium imaging with GECIs, analytical techniques can be employed for clearer reconstruction of firing rates and spike detection (Yaksi and Friedrich 2006; Vogelstein et al., 2009). Therefore, voltage imaging today is limited not by detector technologies, but by the poor properties of the GEVIs, at the same time that most drawbacks of using GECIs lean on the endogenous features of calcium events, which can still benefit from processing tools.

6.3 Spatial discrimination

In response to incoming excitatory inputs, fast depolarizations take place at the neuronal membrane and depending on the intensity or summation of these inputs they can either dissipate or trigger a spike. For the complex computation of such inputs, neurons have efficient mechanisms to distinguish and process the spatial and temporal patterns of the arriving information. In this study, we have successfully used genetically-encoded indicators (exclusively GECIs) to investigate spatial patterns of synaptic inputs (Fig. 9 and 11), and to compare fluorescent readouts originating from EPSPs and evoked APs (Fig. 9 and 10). Moreover we employed them as tool in the study of neuronal synchronization (Fig. 12 and 13).

The attempt to select ROI from different segments of VSFP-expressing neurons turned out to be unsuccessful. It was not possible to collect detectable signals from smaller subcompartments, such as axons and dendrites, because the smaller the membrane selected,

the lower the signal and higher the noise (data not shown). Due to their unsatisfactory properties, VSFPs have not yet been used for other than 'proof-of-principle' experiments. Nevertheless recently released GEVIs generated a great deal of optimism. The development of the probe Arch, for example, has been used to image single action potentials and subthreshold depolarization in cultured neurons (Kralj et al., 2012). Additionally, a novel improved voltage-sensitive indicator, ArcLight, exhibits larger changes in fluorescence in response to voltage changes, detecting individual APs at frequencies up to 16 Hz (highest frequency tested) and allows reliable detection of excitatory potentials in individual dendrites (Jin et al., 2012).

A different feature of calcium imaging is the evident dependence on endogenous buffers and cytoplasmic free calcium. In that regard, most studies performing Ca^{2+} imaging opted to center attention on signals from dendritic line scans only (Mao et al., 2006; Hires et al, 2008). Firstly, because VSCCs and NMDA receptors (main sources of neuronal Ca^{2+} influx) are concentrated along the dendritic plasma membrane (Hille, B. 1992); secondly, because the ratio of membrane surface to the volume of a dendrite is much larger than compared to the soma. Taking also into account that calcium-loaded organelles, such the ER, are found within dendrites, the buffering properties and calcium extrusion taking place in dendrites are much faster and efficient than within the soma.

On the other hand, we decided to analyze and compare SNR derived from soma and dendrites (Fig. 6B, Fig. 9, and Fig. 10). In the first place, for it is at the soma where the summation of synaptic inputs occurs, so that dendritic signals are not necessarily a faithful representation of a neuron's activity. As we show in Figure 10, although a spontaneous AP was recorded using current-clamp, the SNR from a dendrite did not correspond to the expected signal, as was shown from the soma fluorescence response. Furthermore, when recording from larger populations and in *in vivo* preparations, a reduced spatial resolution is available. Therefore, because of the compact nature of dendrites, as well as for the tangled distribution of dendrites in the brain, monitoring of neuronal activity would gain more knowledge if focusing on calcium events from the soma.

6.4 Natural and evoked activity

When neurons are stimulated, calcium enters the cytoplasm through a variety of calcium channels, or is released from the ER (Pozzo-Miller et al., 1999). This fast $[Ca^{2+}]$ elevation is also rapidly brought back to baseline levels via cellular extrusion, storage in

organelles or reloading of intracellular buffers (Hille, 1992). The spatiotemporal evolution of calcium transients is, however, based on two highly distinct sceneries: APs evoked by artificial current injections (antidromic) and spontaneously occurring spikes due to summation of synaptic inputs.

In that regard, whereas the dominant source of antidromic-induced calcium influx is through VSCCs found in the plasma membrane (Jaffe et al., 1992), Ca^{2+} influx coming from synaptic inputs engage different sources, such as NMDA receptors, subtypes of AMPA receptors, internal storages, as well as VSCCs (Higley & Sabatini, 2008). Calcium transients resulting from these processes clearly recruit diverse cell-surface ion channels and are likely to achieve different ranges of calcium accumulations (Jaffe et al., 1992). For that dynamic feature, GCaMP variants have been subcellularly targeted to the pre-synapse (Mao et al., 2008; Dreosti et al., 2009) and to the membrane (Shigetomi et al., 2010), to detect such variations on a more accurate manner.

In Figure 11 we compared evoked APs with naturally occurring EPSPs and our findings corroborate this diversity on calcium fluctuations. This direct calcium imaging illustrates that calcium responses during antidromic spikes are not linear and that synaptic calcium signals from dendrites and spines are not linear nor proportional to full APs. Indeed, changes in $[Ca^{2+}]$ dependent on activity has been widely shown to fluctuate not-linearly (Scheuss et al., 2006) as it is shaped by the type, the quantity and localization of synaptic inputs, as well as mobility and kinetics endogenous buffering proteins that can be cell- and subcompartment-specific.

7 CONCLUSION

Our comparison of the three genetically-encoded indicators allowed a better understanding on many sides of the application of such proteins to the study of neuronal activity. We encountered indicatives that physiological disturbances can occur in expressing-neurons, such as seen within the group expressing VSFP1.2. Moreover, in our experimental conditions we observed that the expression of the probes itself does not necessarily mean that they properly function in response to neuronal activity. Therefore, our findings indicate that reliable standardizations and consistent controls must be primarily established in order to employ such tools in a trustworthy conduct.

In experiments where interests consist of accurate detections of spikes, the application of the reporters studied here will still require the benefits from traditional patch-clamp recordings. As we showed, at 10 Hz only half of the APs could be reliably distinguished with the fluorescence evoked responses. In studies where sparse spikes or synaptic activity are the focus, our results indicate that the available calcium indicators allow detailed studies on neuronal communication, ranging from individual dendritic spines to the investigation of events of synchrony in neuronal networks of genetically defined populations. In contrast, VSFPs are still to be improved, but represent a promising technology for monitoring neural activity, since neurons work on a time scale much faster than calcium events can predict.

Therefore, the miscellaneous collection of activity indicators at our disposal should hereafter be combined, so that, by contemplating the unveiled neuronal networks, our curiosity will pursue to shed light on dissecting our circuit-based, intricate brain.

8 REFERENCES

Adams, F. (1886). The Genuine Works of Hippocrates, Vol. 2, 344-5.

Akemann, W., Mutoh, H., Perron, A., Rossier, J., and Knöpfel, T. (2010). Imaging brain electric signals with genetically targeted voltage-sensitive fluorescent proteins. Nat Methods, 7, 643-9.

Akemann, W., Mutoh, H., Perron, A., Kyung Park, Y., Iwamoto, Y., et al.. (2012). Imaging Neural Circuit Dynamics with a Voltage-Sensitive Fluorescent Protein. J Neurophysiol. 108(8):2323-37

Akerboom, J., Chen, T.W., Wardill, T.J., Tian, L., Marvin, J.S., et al. (2012). Optimization of a GCaMP Calcium Indicator for Neural Activity Imaging. J Neurosci 32: 13819–13840.

Arieli, A., Shoham, D., Hildesheim, R., and Grinvald, A. (1995).Coherent spatio-temporal pattern of on-going activity revealed by real time optical imaging coupled with single unit recording in the cat visual cortex. J. Neurophysiol. 73, 2072–2093.

Banks, M. I. and. Pearce, R A. (2000). Kinetic Differences between Synaptic and Extrasynaptic GABAA Receptors in CA1 Pyramidal Cells. The Journal of Neuroscience, 20(3):937–948.

Berger, T., Borgdorff, A., Crochet, S., Neubauer, F.B., Lefort, S., et al. (2007). Combined voltage and calcium epifluorescence imaging in vitro and in vivo reveals subthreshold and suprathreshold dynamics of mouse barrel cortex. J. Neurophysiol. 97, 3751–3762.

Bianchi, R., and Wong, R.K. (1994). Carbachol-induced synchronized rhythmic bursts in CA3 neurons of guinea pig hippocampus in vitro. J Neurophysiol.;72(1):131-8.

Borgius, L., Restrepo, C. E., Leão, R. N., Saleh, N., Kiehn, O. (2010). A transgenic mouse line for molecular genetic analysis of excitatory glutamatergic neurons. Mol Cell Neurosci 45, 245-257.

Bradley, J., Luo, R., Otis, T. S. , and DiGregorio, D. A. Submillisecond optical reporting of membrane potential in situ using a neuronal tracer dye. J. Neurosci. 29, 9197–9209 (2009)

Buzsáki, G. (2004). Large-scale recording of neuronal ensembles. Nature Neurosci. 7, 446–451.

Buzsáki, G., Anastassiou, C. A., and Koch, C. (2012).The origin of extracellular fields and currents - EEG, ECoG, LFP and spikes. Nature Rev. Neurosci. 13, 407–420.

Chen, Q., Cichon, J., Wang, W., Qiu, L., Lee, S.R., Campbell, N.R, DeStefino, N., Goard, M.J., Fu, Z., Yasuda, R., Looger, L.L., Arenkiel, B.R., Gan, W. and Feng, G. (2012). Imaging neural activity using Thy1-GCaMP transgenic mice Neuron 76, 297–308.

Chudakov, D. M., Matz, M. V., Lukyanov S., and Lukyanov, K. A. (2010) Fluorescent proteins and their applications in imaging living cells and tissues. Physiol Rev, 90, 1103-63.

Daya, R.N, and Davidson, M.W. (2009). The fluorescent protein palette: tools for cellular imaging. Chem Soc Rev. 38(10): 2887–2921

DeFelipe, Javier. Cajal's butterflies of the soul. Science and Art; Oxford, 2010

Dimitrov, D., He, Y., Mutoh, H., Baker, B. J., Cohen, L., et al. (2007). Engineering and characterization of an enhanced fluorescent protein voltage sensor. PLoS One, 2, e440.

Dixit, R. and Cyr, R. (2003). Cell damage and reactive oxygen species production induced by fluorescence microscopy: effect on mitosis and guidelines for non-invasive fluorescence microscopy", The Plant Journal, 36: 280-290.

Dombeck, D. A., Khabbaz, A. N., Collman, F., Adelman, T. L. , and Tank, D. W. (2007). Imaging large-scale neural activity with cellular resolution in awake, mobile mice. Neuron 56, 43–57.

Dreosti, E., B. Odermatt, M.M. Dorostkar, L. Lagnado. (2009). A genetically encoded reporter of synaptic activity in vivo Nature Methods, 6 883-U122

Einevoll, G. T., Franke, F., Hagen, E., Pouzat, C., and Harris, K. D. (2012).Towards reliable spike-train recordings from thousands of neurons with multielectrodes. Curr. Opin. Neurobiol. 22, 11–17

Ferezou, I., Bolea, S., Petersen, C.C. (2006). Visualizing the cortical representation of whisker touch: voltage-sensitive dye imaging in freely moving mice. Neuron 50: 617–629.

Ferezou, I., Haiss, F., Gentet, L.J., Aronoff, R., Weber, B. et al. (2007). Spatiotemporal dynamics of cortical sensorimotor integration in behaving mice. Neuron 56: 907–923.

Fetcho JR, Cox KJ, O'Malley DM. (1998). Monitoring activity in neuronal populations with single-cell resolution in a behaving vertebrate. Histochem J 30: 153–167.

Fukuda, S., Kato, F., Tozuka, Y., Yamaguchi, M., Miyamoto, Y., et al. (2003). Two distinct subpopulations of nestin-positive cells in adult mouse dentate gyrus. J Neurosci 23: 9357–9366.

García-Lopez, P., García-Marín, V., and Freire, M. (2007). The discovery of dendritic spines by Cajal in 1888 and its relevance in the present neuroscience. Progress in Neurobiology 83; 110-130.

Grinvald, A. , and Hildesheim, R. VSDI: a new era in functional imaging of cortical dynamics. (2004). Nature Rev. Neurosci. 5, 874–885.

Halliwell, B., and Gutteridge, J. M. C. (1989). Free radicals in biology and medicine, Oxford: Claredon Press.

Hamill, O. P., Marty, A., Neher, E., Sakmann, B. , and Sigworth, F. J. (1981). Improved patch-clamp techniques for high-resolution current recording from cells and cell-free membrane patches. Pflügers Arch. 391, 85–100.

Harris, D. C. (2010). Applications of Spectrophotometry. Quantitative Chemical Analysis (8th ed.). New York: W. H. Freeman and Co. pp. 419–44.

Heim, N., and Griesbeck, O. (2004) Genetically encoded indicators of cellular calcium dynamics based on troponin C and green fluorescent protein. J Biol Chem 279: 14280–14286.

Higley MJ, and Sabatini BL (2008). Calcium signaling in dendrites and spines: practical and functional considerations. Neuron 59(6):902-13

Hille B. (1992). Pumping ions. Science 255: 742.

Hires, S.A., Tian L., and Looger, L.L. (2008). Reporting neural activity with genetically encoded calcium indicators. Brain Cell Biol; 36(1-4): 69–86.

Hodgkin A.L., Huxley A.F. (1939). Action potentials recorded from inside a nerve fibre. Nature 144:710–711

Hodgkin, A.L., and Huxley, A.F. (1952)a. The components of membrane conductance in the giant axon of Loligo. J Physiol 116:473–496

Hodgkin, A.L., and Huxley, A.F. (1952)b. Currents carried by sodium and potassium ions through the membrane of the giant axon of Loligo. J Physiol 116:449–472

Hodgkin, A. L., and Huxley, A. F. (1952)c. A quantitative description of membrane current and its application to conduction and excitation in nerve. J. Physiol. (Lond.) 117, 500–544

Horikawa, K., Y. Yamada, T. Matsuda, K. Kobayashi, M. Hashimoto, T. et al. (2010). Spontaneous network activity visualized by ultrasensitive Ca(2+) indicators, yellow Cameleon-Nano. Nat Methods, 7, 729-32.

Jaffe, D.B., Johnston, D., Lasser, R.N., Lisman, J.E., Miyakawa, H., et al. (1992). The spread of Na+ spikes determines the pattern of dendritic Ca2+ entry into hippocampal neurons. Nature 357: 244–246.

Ji, N., Shroff, H., Zhong, H., and Betzig, E. (2008). Advances in the speed and resolution of light microscopy. Curr. Opin. Neurobiol. 18, 605–616.

Jin, L., Han, Z., Platisa, J., Wooltorton; J. R. A., Cohen, L. B., et al. (2012). Single action potentials and subthreshold electrical events imaged in neurons with a novel fluorescent protein voltage probe Neuron; 75(5): 779–785

Knöpfel, T. (2012). Genetically encoded optical indicators for the analysis of neuronal circuits. Nature Reviews Neuroscience 13, 687-700’

Knöpfel, T., Díez-García , J. and Akemann, W. (2006). Optical probing of neuronal circuit dynamics: genetically encoded versus classical fluorescent sensors. Trends Neurosci, 29, 160-6.

Knöpfel, T., M. Z. Lin, A. Levskaya, L. Tian, J. Y. Lin , and E. S. Boyden (2010) Toward the second generation of optogenetic tools. J Neurosci, 30, 14998-5004.

Kole, M.H.P. (2011). First Node of Ranvier Facilitates High-Frequency Burst Encoding. Neuron 71, 569-570.

Kralj, J. M., Douglass, A. D., Hochbaum, D. R., Maclaurin, D. , and Cohen, A. E. (2012).Optical recording of action potentials in mammalian neurons using a microbial rhodopsin. Nature Methods 9, 90–95.

Kremers, G., Gilbert, S.G., Cranfill, P.J., Davidson, M.W. and Piston, D.W. (2011). Fluorescent proteins at a glance. Cell Sci. 124, 157-160.

Lapray, D. (2012). Behavior-dependent specialization of identified hippocampal interneurons. Nature Neuroscience, 15, 1265–1271.

Leão, R.N., Mikulovic, S., Leão, K.E., Munguba, H., Gezelius, H., et al. (2012). OLM interneurons differentially modulate CA3 and entorhinal inputs to hippocampal CA1 neurons. Nat Neurosci. 2012 Nov;15(11):1524-30

Lee, A. K., Manns, I. D., Sakmann, B. and Brecht, M. (2006).Whole-cell recordings in freely moving rats. Neuron 51, 399–407.

Lütcke, H., Murayama, M., Hahn, T., Margolis, D.J., Astori, S., et al. (2010). Optical recording of neuronal activity with a genetically-encoded calcium indicator in anesthetized and freely moving mice. Front Neural Circuits 4:9.

Maeda,H., Ellis-Davies, G.C.R., Ito, K., Miyashita,Y., and Kasai, H. (1999). Supralinear Ca2+ signaling by cooperative and mobile Ca2+ buffering in Purkinje neurons. Neuron 24, 989–1002.

Mah, S.J., Fleck, M.W., and Lindsley T.A. (2011). Ethanol alters calcium signaling in axonal growth cones. Neuroscience, 189, 384–396.

Mank, A. F., Santos, S., Direnberger, T. D., Mrsic-Flogel, S. B., Hofer, V et al (2008). A genetically encoded calcium indicator for chronic in vivo two-photon imaging. Nat Methods. 5, 805 - 811

Mank M, and Griesbeck O. (2008). Genetically encoded calcium indicators. Chem Rev.; 108:1550–1564.

Mao, T, O'Connor, D.H., Scheuss, V., Nakai, J. Svoboda, K. (2008) Characterization and Subcellular Targeting of GCaMP-Type Genetically-Encoded Calcium Indicators, (3), 3, e1796

Markram, H., Helm, P.J., and Sakmann, B. (1995).Dendritic calcium transients evoked by single back-propagating action potentials in rat neocortical pyramidal neurons. J. Physiol 485(Pt 1),1–20.

Miyawaki, A., and Tsien, R.Y. (2000). Monitoring protein conformations and interactions by fluorescence resonance energy transfer between mutants of green fluorescent protein. Methods Enzymol 327: 472–500.

Morise, H., Shimomura, O., Johnson, F.H., and Winant, J. (1974). Intermolecular energy transfer in the bioluminescent system of Aequorea. Biochemistry.;13(12):2656-62

Mutoh, H., and Knöpfel, T. (2013). Probing neuronal activities with genetically encoded optical indicators: from a historical to a forward-looking perspective. Eur J Physiol.

Mutoh, H., Perron, A., Akemann, W., Iwamoto, Y., and Knöpfel, T. (2011). Optogenetic monitoring of membrane potentials Exp Physiol January 1, 96 (1) 13-18

Mutoh, H., Perron, A., Dimitrov, D., Iwamoto, Y., Akemann, W. et al. (2009). Spectrally-resolved response properties of the three most advanced FRET based fluorescent protein voltage probes. PLoS One, 4, e4555.

Neher, E., and Sakmann, B. (1976) Single-channel currents recorded from membrane of denervated frog muscle fibres. Nature 260:799–802

Kuczewski, N., Porcher, C., Ferrand, N., Fiorentino, H., Pellegrino, C., et al. (2008). Backpropagating Action Potentials Trigger Dendritic Release of BDNF during Spontaneous Network Activity. The Journal of Neuroscience, 28(27): 7013-7023-

Nimchinsky, E. A., Sabatini, B. L., and Svoboda, K. (2002). Structure and function of dendritic spines. Annu. Rev. Physiol. 64, 313–353

Palmer, A.E., and Tsien, R.Y. (2006). Measuring calcium signaling using genetically targetable fluorescent indicators. Nat Protoc 1: 1057–1065.

Perin, R., Berger, T. K. , and Markram, H. (2011). A synaptic organizing principle for cortical neuronal groups. Proc. Natl Acad. Sci. USA 108, 5419–5424

Perron, A., H. Mutoh, W. Akemann, S. G. Gautam, D. Dimitrov, et al. (2009). Second and third generation voltage-sensitive fluorescent proteins for monitoring membrane potential. Front Mol Neurosci, 2, 5.

Perron, A., Akemann, W., Mutoh, H., and Knöpfel, T. (2012). Genetically encoded probes for optical imaging of brain electrical activity. Prog Brain Res, 196, 63-77.

Polley, D. B., Kvasnak, E., and Frostig, R. D. (2004). Naturalistic experience transforms sensory maps in the adult cortex of caged animals. Nature 429, 67–71

Pozzo-Miller, L.D., Pivovarova, N.B., Connor, J.A., Reese, T.S., and Andrews, B. (1999). Correlated measurements of free and total intracellular calcium concentration in central nervous system neurons. Mic Res Tech 46: 370–379.

Prasher, D. C., Eckenrode, V. K., Ward, W. W., Prendergast, F. G. and Cormier, M. J. (1992). Primary structure of the Aequorea victoria green-fluorescent protein. Gene 111, 229-233.

Ramón y Cajal, S. (1917). Recuerdos de mi vida, Vol. 2. Historia de mi labor cientifica. Madrid: Moya.

Romoser, V. A., Hinkle, P. M., and Persechini, A. (1997). Detection in living cells of Ca2+-dependent changesin the fluorescence emission of an indicator composed of two green fluorescent protein variants linked by a calmodulin-binding sequence. A new class of fluorescent indicators. J. Biol. Chem. 272, 13270–13274.

Rouach, N., Segal, M., Koulakoff, A., Giaume, C., and Avignone E. (2003). Carbenoxolone blockade of neuronal network activity in culture is not mediated by an action on gap junctions. J Physiol (2003), 553.3, pp. 729–745

Ryge, J., Westerdahl, A.C., Alstrøm, P., and Kiehn, O. (2008). Gene expression profiling of two distinct neuronal populations in the rodent spinal cord. PLoS One.; 3(10) e3415.

Sabatini, B. L., and Svoboda, K. (2000). Analysis of calcium channels in single spines using optical fluctuation analysis. Nature 408, 589–593.

Salzberg, B. M., Obaid, A. L., Senseman, D. M. , and Gainer, H. (1983). Optical recording of action potentials from vertebrate nerve terminals using potentiometric probes provides evidencefor sodium and calcium components. Nature 306, 36–40.

Scanziani, M , and Häusser, M. (2009). Electrophysiology in the age of light. Nature 461; 930-939.

Scheuss, V., Yasuda, R., Sobczyk, A., and Svoboda, K. (2006) Nonlinear [Ca2+] signaling in dendrites and spines caused by activity-dependent depression of Ca2+ extrusion. J Neurosci 26: 8183–8194.

Shaner, N. C., Lin, M. Z., McKeown, M. R., Steinbach, P. A., Hazelwood, K. L., et al. (2008). Improving the photostability of bright monomeric orange and red fluorescent proteins. Nature Methods 5, 545-551.

Shcherbo, D., Murphy, C. S., Ermakova, G. V.,Solovieva, E. A., Chepurnykh, T. V., et al. (2009). Far-red fluorescent tags for protein imaging in living tissues. Biochem. J. 418, 567-574.

Shigetomi, E., Kracun, S., Sofroniew, M.V., and Khakh, B.S. (2010). A genetically targeted optical sensor to monitor calcium signals in astrocyte processes. Nature Neuroscience, 13. 759-U143

Shimomura, O., Johnson, F. H., and Saiga, Y. (1962). Extraction, purification and properties of aequorin, a bioluminescent protein from the luminous hydromedusan, Aequorea. J. Cell Comp. Physiol. 59, 223-239.

Siegel, M. S. and Isacoff, E. Y. (1997). A genetically encoded optical probe of membrane voltage. Neuron 19, 735–741.

Slovin, H., Arieli, A., Hildesheim, R., and Grinvald, A. (2002). Long-term voltage-sensitive dye imaging reveals cortical dynamics in behaving monkeys. J Neurophysiol 88: 3421–3438.

Svoboda, K., Denk, W., Kleinfeld, D., and Tank, D.W. (1997). In vivo dendritic calcium dynamics in neocortical pyramidal neurons. Nature 385: 161–165.

Tasaki, I., Watanabe, A., Sandlin, R., and Carnay, L. (1968).Changes in fluorescence, turbidity and birefringence associated with nerve excitation. Proc. Natl Acad. Sci. USA 61, 883–888.

Tian, L., Hires, S.A., and Looger, L.L. (2012). Imaging neuronal activity with genetically encoded calcium indicators Cold Spring Harb Protoc (6):647-56.

Tian, L., Hires, S.A., Mao, T., Huber, D., Chiappe, M.E., et al. (2009). Imaging neural activity in worms, flies and mice with improved GCaMP calcium indicators. Nat Methods 6:875–881.

Tian, L., and L. L. Looger (2008) Genetically encoded fluorescent sensors for studying healthy and diseased nervous systems. Drug Discov Today Dis Models, 5, 27-35.

Tour, O., Adams, S.R., Kerr, R.A., Meijer, R.M., Sejnowski, T.J., et al. (2007). Calcium Green FlAsH as a genetically targeted small-molecule calcium indicator. Nat Chem Biol 3: 423–431

Tsien, R. Y. (1998). The green fluorescent protein. Annu. Rev. Biochem. 67, 509-544.

Verkhratsky, A., Krishtal, O. A., and Petersen, O. H. (2006). From Galvani to patch clamp: the development of electrophysiology, European Journal of Physiology. 453:233–247

Vogelstein, J.T., Watson, B.O., Packer, A.M., Yuste, R., Jedynak, B., et al. (2009). Spike inference from calcium imaging using sequential Monte Carlo methods.

Wallace, D.J., Meyer A. B. S., Astori, S., Yang, Y., Bausen, M., et al (2008). Single-spike detection in vitro and in vivo with a genetic Ca2+ sensor. Nat Methods 5: 797–804.

Wright, W. A., Bubb, C., Hawkins, L., and Davies, M. J. (2002). Singlet oxygenmediated protein oxidation: evidence for the formation of reactive side chain peroxides of tyrosine residues, Photochem. Photobiol, 76: 35-46.

Yaksi, E., and Friedrich, R.W. (2006). Reconstruction of firing rate changes across neuronal populations by temporally deconvolved Ca2+ imaging. Nat Methods 3: 377–383.

Yamada, Y., and Mikoshiba, K. (2012). Quantitative comparison of novel GCaMP-type genetically encoded Ca2+ indicators in mammalian neurons. Front. Cell. Neurosci. 6:41.

Yamada, Y., Michikawa, T., Hashimoto, M., Horikawa, K., Nagai, T., et al. (2011). Quantitative comparison of genetically encoded Ca indicators in cortical pyramidal cells and cerebellar Purkinje cells. Front Cell Neurosci 5, 18.

Zariwala HA, Borghuis BG, Hoogland TM, Madisen L, Tian L, De Zeeuw CI, Zeng H, Looger LL, Svoboda K, Chen TW (2012) A Cre-dependent GCaMP3 reporter mouse for neuronal imaging in vivo. J Neurosci32:3131–3141.

Zhang, F., Prigge, M., Beyriere, F., Tsunoda, S.P., Mattis, J., et al. (2008). Red-shifted optogenetic excitation: a tool for fast neural control derived from Volvox carteri. Nat Neurosci 11, 631–633.

Zhao, Y., Araki, S., Wu, J., Teramoto, T., Chang, Y. F., et al. (2011) An expanded palette of genetically encoded Ca^{2+} indicators. Science, 333, 1888-91.